
Dynamics and Spectroscopy of Molecular Processes in Solid Hydrogen

R.B. Gerber

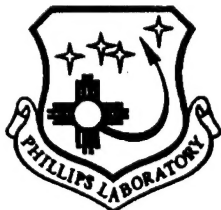
University of California Irvine
Department of Chemistry
Irvine, CA 92717

August 1996

19961029 090

Final Report

APPROVED FOR PUBLIC RELEASE; DISTRIBUTION UNLIMITED



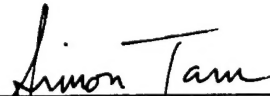
PHILLIPS LABORATORY
Propulsion Directorate
AIR FORCE MATERIEL COMMAND
EDWARDS AIR FORCE BASE CA 93524-7048

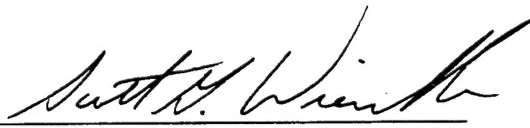
DEES QUALITY INSPECTED 1

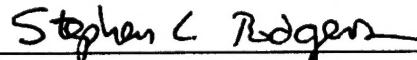
FOREWORD

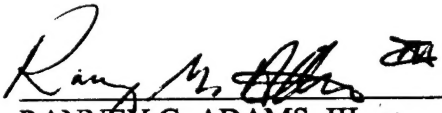
This final technical report was prepared by the University of California Irvine, Irvine, CA 92717, under Contract F29601-92-K-0016 with the OL-AC, Phillips Laboratory, Edwards AFB CA 93524-7048. Project Manager for Phillips Laboratory was Simon Tam.

This report has been reviewed and is approved for release and distribution in accordance with the distribution statement on the cover and on the SF Form 298.


SIMON TAM
Project Manager


SCOTT G. WIERSCHKE, Capt, USAF
Deputy Director
Propulsion Sciences


STEPHEN L. RODGERS
Director
Propulsion Sciences


RANNEY G. ADAMS, III
Public Affairs Director
OLAC, PL/PAS 96-136

REPORT DOCUMENTATION PAGE			Form Approved OMB No 0704-0188	
Public reporting burden for this collection of information is estimated to average 1 hour per response, including the time for reviewing instructions searching existing data sources gathering and maintaining the data needed, and completing and reviewing the collection of information. Send comments regarding this burden estimate or any other aspect of this collection of information, including suggestions for reducing this burden to Washington Headquarters Services, Directorate for Information Operations and Reports, 1215 Jefferson Davis Highway, Suite 1204, Arlington, VA 22202-4302, and to the Office of Management and Budget, Paperwork Reduction Project (0740-0188), Washington DC 20503.				
1. AGENCY USE ONLY (LEAVE BLANK)		2. REPORT DATE August 1996		3. REPORT TYPE AND DATES COVERED Final Report
4. TITLE AND SUBTITLE Dynamics and Spectroscopy of Molecular Processes in Solid Hydrogen			5. FUNDING NUMBERS C: F29601-92-K-0016 PE: 62601F PR: 3058 TA: 00EN	
6. AUTHOR(S) Gerber, R.B.				
7. PERFORMING ORGANIZATION NAME(S) AND ADDRESS(ES) University of California Irvine Department of Chemistry Irvine CA 92717			8. PERFORMING ORGANIZATION REPORT NUMBER	
9. SPONSORING/MONITORING AGENCY NAME(S) AND ADDRESS(ES) Phillips Laboratory OLAC PL/RKS 10 East Saturn Drive Edwards AFB CA 93524-7680			10. SPONSORING/MONITORING AGENCY REPORT NUMBER PL-TR-96-3013	
11. SUPPLEMENTARY NOTES COSATI CODE(S): 20/13; 07/04;				
12a. DISTRIBUTION/AVAILABILITY STATEMENT Public Release; Distribution Unlimited			12b. DISTRIBUTION CODE A	
13. ABSTRACT (MAXIMUM 200 WORDS) <p>The general objective of this research was to determine by theoretical simulations dynamic properties of solid hydrogen clusters, doped with certain atoms, such as boron, magnesium and lithium. Doped solid hydrogen systems are of great interest as potentially advanced propellants of high specific impulse. As such, knowledge of the properties of such systems is of major importance for the Air Force project on High Energy Density Materials (HEDM). Also, doped solid hydrogen and doped hydrogen clusters are of basic scientific interest, since such systems are expected to exhibit strong quantum mechanical effects.</p> <p>A novel method was developed for time-dependent quantum simulations of large systems. The method is, to the author's knowledge, a unique tool, to date, for quantum simulations in time of processes in many-atom systems. Applications for realistic systems having up to ~50 atoms are at hand, extensions to much larger systems are underway. The method has a wide range of potential applications for HEDM systems, e.g., doped solid hydrogen, for cryogenic systems in general, and also for other molecular systems. Preliminary applications are described in the report.</p> <p>Another time-dependent simulation method, based on the Time-Dependent Self-Consistent Field (TDSCF) approximation, was also developed and tested for quantum clusters. Not as efficient and widely applicable in general as method (1) above, the TDSCF-based algorithm was found to have a useful "niche" of applications for cryogenic materials where quantum effects are moderate, such as solid Ne, or solid H₂ at high pressures. This result also contributes to the accomplishment of Task 7 of the Program Plan.</p>				
14. SUBJECT TERMS molecular dynamics; time-dependent quantum simulations; quantum Monte Carlo simulations, HEDM; solid hydrogen; propellants			15. NUMBER OF PAGES 51	
			16. PRICE CODE	
17. SECURITY CLASSIFICATION OF REPORT Unclassified	18. SECURITY CLASSIFICATION OF THIS PAGE Unclassified	19. SECURITY CLASSIFICATION OF ABSTRACT Unclassified	20. LIMITATION OF ABSTRACT SAR	

List of Figures

<u>Figure</u>	<u>Page</u>
1 Time Evolution of the Ba-Ar Atom-Atom Distribution Function for the Ba(Ar) ₁₀ Cluster	8
2a Branching Ratios for the S-Type and the Two P-Type Excited States of the Ba(Ar) ₁₀ Cluster	10
2b Branching Ratios for the S-Type and the Two P-Type Excited States of the Ba(Ar) ₁₀ Cluster	11
3 The Ne-Ne Distance Distribution Function for (Ne) ₁₃ at T=1K. Semi-Classical Molecular Dynamics Results are Compared with Feynman Path Integral Simulations. From Ref. (22)	15
4 The Accretion Energies (Right Panel) and Solvation Energies (Left Panel) of B(H ₂) _n as a Function of <i>n</i>	19
5 The Structures of Global and Local Minima of Clusters B(H ₂) _n	20
6 Structural Distribution for B(H ₂) _n from DQMC	21
7 The H ₂ -Hg Distance Distribution in the Ground State of Hg(H ₂) ₁₂	23
8 The H ₂ -H ₂ Distance Distribution in the Ground State of Hg(H ₂) ₁₂	24
9 The H ₂ -Mg Distance Distribution in the Ground State of Mg(H ₂) ₁₂	25
10 The H ₂ -H ₂ Distance Distribution in the Ground State of Mg(H ₂) ₁₂ (From DQMC)	26
11 The Mg-H ₂ Distance Distribution of the Mg(H ₂) ₁₂ at T=2K and at T=4K	27
12 The H ₂ -H ₂ Distance Distribution for Mg(H ₂) ₁₂ at T=2K and at T=4K	28
13 Density Contours for H ₂ Molecules in a Plane Containing the Center of Mg, for the Cluster Mg(H ₂) ₁₂ at T=0K	29
14a Snapshot of the Time Evolution of the Wave Packet of Li*(H ₂) ₂ After Photexcitation. t=0.0 fs	32
14b Snapshot of the Time Evolution of the Wave Packet of Li*(H ₂) ₂ After Photoexcitation. t=3600 fs	32

List of Figures (cont.)

<u>Figure</u>		<u>Page</u>
14c	Snapshot of the Time Evolution of the Wave Packet of $\text{Li}^*(\text{H}_2)_2$ After Photoexcitation. $t=7200$ fs	33
14d	Snapshot of the Time Evolution of the Wave Packet of $\text{Li}^*(\text{H}_2)_2$ After Photoexcitation. $t=14400$ fs	33
15	Final Vibrational State Distribution of the Dissociation Fragment $\text{Li}^* - \text{H}_2$ After the Photoexcitation	34
16	The Probability for Cluster Survival in Collinear Collisions of Li Atoms with $(\text{H}_2)_2$ and $(\text{D}_2)_2$	35
17	The Survival Probability of $\text{B}-\text{H}_2$ in Collinear Collisions with (H_2) Molecules	35

List of Tables

<u>Table</u>		
1	DQMC Results for the Cohesion Energy of Quantum Clusters	16
2	Calculated Potential Energy Minima and Lowest Vibrational Energies of $\text{B}(\text{H}_2)_n$	18

1. INTRODUCTION: Research Objectives and Summary of the Results

1.1 Aims of the Research

The general objective of this research was to determine by theoretical simulations dynamical properties of solid hydrogen clusters, doped with certain atoms, such as boron, magnesium and lithium. Doped solid hydrogen systems are of great interest as potentially advanced propellants of high Specific Impulse. (Ref. 1) As such, knowledge of the properties of such systems is of major importance for the Air Force project on High Energy Density Materials (HEDM). Also, doped solid hydrogen and doped hydrogen clusters are of basic scientific interest, since such systems are expected to exhibit strong quantum mechanical effects. The properties targeted in the proposal involved time-dependent phenomena and processes. An objective of central importance of the research was the development of methods and algorithms for the simulation of time-dependent behavior in low-temperature systems exhibiting strong effects. The challenge here is to develop a novel computational method for solving the quantum-mechanical time-dependent Schrödinger equation for many-atom systems. This goal, described as Task 7 of the original Program Plan, was essential for constructing a tool of simulation for the purposes of this proposal, but clearly if attained it provides a powerful means also for future studies of many other properties of low-temperature, highly quantum-mechanical systems. One of the applications targeted in this proposal was the description of the dynamics following excitation of a metal atom in a solid hydrogen environment, or in hydrogen clusters. This is important for the spectroscopic characterization of the system. This is the content of Tasks 6 and 8 of the original proposal. Another important time-dependent property is the dynamical stability of the system. One of the objectives of the proposal (Task 5 of the revised Work Plan) was to calculate collisions of doped hydrogen clusters with atoms and molecules, and determine their survival probability. This information is important for some of the methods for preparing doped hydrogen systems. To fully characterize doped hydrogen systems, structural and energetic properties must be described, in addition to the time-dependent behavior. One of the key objectives of the proposal was to determine by quantum-mechanical simulations the structural and energetic properties of various doped hydrogen clusters (Task 1 and Task 4 of the original workplan). Another objective was to determine the stability of doped hydrogen systems against diffusion (Task 3 of the Work Plan). In summary, the main aims of this proposal were to develop simulation methods for many-atom quantum systems, and to carry out calculations for several time-dependent properties, as well as for related structural and energetic properties of doped hydrogen systems.

1.2 Brief Summary of the Research Results

In the course of the research project described in this report, the following main results were obtained:

(1) A novel method was developed for time-dependent quantum simulations of large systems. The method is, to the author's knowledge, a unique tool to date for quantum simulations in time of processes in many-atom systems. Applications for realistic systems having up to ~ 50 atoms are at hand, extensions to much larger systems are under way. The method has a wide range of potential applications for HEDM systems, e.g. doped solid hydrogen, for cryogenic systems in general, and also for other molecular systems. Preliminary applications are described in the report. (Refs. 2-4) This development

successfully accomplishes Task 7 of the original Program Plan. The author regards this as the most important result of this project.

(2) Another time-dependent simulation method, based on the Time-Dependent Self-Consistent Field (TDSCF) approximation, was also developed and tested for quantum clusters. Not as efficient and widely applicable in general as method (1) above, the TDSCF-based algorithm was found to have a useful "niche" of applications for cryogenic materials where quantum effects are moderate, such as solid Ne, or solid H_2 at high pressures. This result also contributes to the accomplishment of Task 7 of the Program Plan.

(3) The structural and energetic properties of $B(H_2)_n$ clusters, $n \leq 8$, were studied by Diffusion Quantum Monte Carlo (DQMC) simulations (cooperation with Prof. M.H. Alexander). For the smaller clusters, the structures are planar, with the H_2 molecules located normal to the p orbital of the boron atom. The B atom is solvated inside a ring of H_2 molecules, for $n \geq 6$; that is, the boron is encircled by the hydrogen, and stabilized in this way. The binding energy is much higher than for neat $(H_2)_n$ clusters. In the solid one therefore expects a strong cluster involving the B atom and at least 6 neighboring H_2 molecules. This should be stable up to the melting point of solid hydrogen. Since the B atom is strongly bound to neighboring H_2 molecules, the diffusivity of B in solid H_2 is predicted to be extremely low. This (together with corresponding results for $Mg(H_2)_n$ clusters) accomplishes Tasks 1 and 4 of the updated Program Plan.

(4) The predicted "solvation" of B atoms in H_2 , and the strong clustering of atoms with several neighboring H_2 molecules with resulting low diffusivity even for temperatures well above 4K, suggest that an appreciable concentration of B atoms (several percent) in solid hydrogen should be fairly stable. By these results, boron in hydrogen appears a very promising HEDM material, far superior to any other system studied in this project.

(5) Structural and energetic properties of $Mg(H_2)_n$ clusters, with $n \leq 18$, were studied by DQMC. In the ground state, which the DQMC computes, the magnesium is solvated inside a shell of H_2 molecules. The shell is not isotropic for any cluster size, and can be roughly described as an anisotropic quantum liquid. However, the Mg atom cannot be found at or beyond the H_2 shell with any significant probability, so it is "shielded" inside the H_2 shell. This (together with the above results for boron, and with (6) below) accomplishes Tasks 1 and 4.

(6) Using Feynman Path Simulations, structural properties of $Mg(H_2)_n$ at thermal equilibrium were calculated for different temperatures. It was found that the Mg remains solvated inside the shell of H_2 , for $12 \leq n$, up to the evaporation point of the cluster, around 4.2K. On this basis, diffusion of Mg in solid hydrogen is expected to be very low under 4K. This, together with previous results above, accomplishes Tasks 1, 4.

(7) Mg in hydrogen has properties useful for HEDM by our results, though not as advantageous as those of B in H_2 . The low diffusivity below 4K, due to the solvation effect, suggests that Mg in appreciable concentrations in hydrogen can remain stable at low temperatures. Mg seems much superior in this respect to Lithium in hydrogen.

(8) The ground-state vibrational wavefunction of $Mg(H_2)_n$ is highly delocalized. The $Mg-H_2$ distance distribution covers relative distances from $\sim 2.5\text{\AA}$ to $\sim 7.0\text{\AA}$. In the larger clusters, $n \geq 10$, the computed wavefunction suggests "radial" vibrations of the H_2 with respect to the Mg, and collective vibrations of the hydrogens on a near-spherical shell. The characterization of the vibrational wavefunction of $Mg(H_2)_n$ accomplishes

(together with (9) below), Task 2.

(9) The ground-state vibrational wavefunction of $B(H_2)_n$ is also very delocalized, although the relative $B-H_2$ distance distribution is less spread out than the $Mg-H_2$ one (the range of distances is $3\text{\AA} - 5\text{\AA}$, roughly). The mean structure, say of $B(H_2)_6$, is planar, but the out of plane zero-point structural fluctuations are very large. This characterization of the vibrational motion accomplishes part of Task 2 of the Program Plan.

(10) Using time-dependent quantum mechanical methods, collisions of quantum clusters with atoms or with molecules were studied. A surprising and potentially important finding was that survival probabilities of the quantum clusters in such collisions are quite high, despite the low binding energies. For instance, at a collision energy of 150K the survival probability of a $B-H_2$ cluster hit by an H_2 molecule is about 50% ! These results on survival of quantum clusters in collisional impact fulfill Task 5 of the updated Workplan. The results point to possible strategies for the preparation of HEDM materials (such as boron in solid H_2), based on deposition of quantum clusters.

(11) Using a time-dependent quantum algorithm, we calculated the dynamics following electronic excitation of small quantum clusters such as $Li(H_2)_2$. A long lifetime, of the order of 10^4 femtoseconds, was found for the excited state. The channel producing $Li(P) + (H_2)_2$ was found to dominate over the channel resulting in $Li(P) - H_2 + H_2$. The results have applications to characterization of quantum clusters (of HEDM interest) by electronic spectroscopy, including by ultrafast spectroscopic techniques. This calculation attains the goal of Task 6.

(12) The dynamics following electronic excitation of Mg atoms in solid hydrogen was studied by time-dependent quantum simulations, using the novel method developed in this project (item (1) above). The results show coherent cage vibrations, over a time-duration of at least 0.5 fs. Photoinduced mobility of Mg atoms leaving the cage was found. Spectroscopic observables were computed. This calculation accomplishes Task 2, and a large part of Task 8. It demonstrates the power of Quantum Molecular Dynamics simulations using the new method.

(13) Using semiclassical Molecular Dynamics methods, calculations were carried out on the coupled electronic-nuclear motions for Fluorine atoms in solid Kr. This cryogenic system is not of direct HEDM relevance, but is a useful model for P -state open shell atoms in solid H_2 . Both the dynamics at equilibrium, and the dynamics in a photoinduced process, were simulated. The timescales for transitions between electronic states, and for change of electronic polarization (related to electronic orbital reorientation) were computed. The predictions are useful for spectroscopic characterization of HEDM systems such as boron in hydrogen. These results contribute to the accomplishments of Tasks 2 and 8.

(14) In cooperation with experiments at Grenoble, France, by P. Zeppenfeld, O. Wilches and M. Bienfait, (Ref. 5) hydrogen-argon mixed monolayers on graphite were studied. This research, not central to the HEDM issues, is nevertheless important for understanding properties of mixtures in hydrogen with other atoms. The results show that such mixtures are inherently more disordered than corresponding classical mixtures of particles similar in sizes (such as Xe+Kr monolayers). Also, the disordered structures seem to depend on temperature. The results suggest a new type of structural behavior of hydrogen-Ar mixtures in two dimensions, but are still very preliminary.

With the above results listed, all the Tasks set in the original and updated Program Plan have been fully accomplished, with the exception of part of Task 8. The results add significantly to our knowledge on doped hydrogen clusters and solids, on cryogenic systems in general, and possible novel theoretical tools for the description of processes in such systems.

From a HEDM point of view, particularly important findings are those which are very encouraging as to the suitability of boron in hydrogen as a potential HEDM propellant. Also significant are the results on the properties of magnesium in hydrogen: They point to important advantages of this material compared with other metal-hydrogen systems hitherto studied.

2. RESEARCH RESULTS, DATA OBTAINED AND ACCOMPLISHMENTS

2.1 New Method for Time-Dependent Quantum Simulations of Large Systems

2.1.1 Introduction: Classical trajectory simulations have proved a tool of pivotal importance for the understanding of molecular processes in condensed matter as well as in the gas phase. The classical level of description is certainly adequate to a large extent for a great variety of molecular phenomena. This, together with the computational simplicity and power of classical Molecular Dynamics (Ref. 6) have made the latter an extremely useful tool of interpretation and insight, and often also of quantitative prediction. However, in many cases it is desirable to proceed beyond the classical level, to a quantum description. Quantum effects, e.g. non-adiabatic transitions, zero-point motion effects, interference and tunneling have important experimental manifestations. This is relevant to many molecular systems at normal conditions. For systems such as solid hydrogen, quantum effects are very large, and the ability to treat them in simulations is of critical importance. HEDM systems such as doped solid hydrogen are clearly in this category. Hence a very central goal of the research reported here was to develop a method for time-dependent quantum-mechanical simulations of systems having many atoms. This is Task No. 7 of the Program Plan of our project - essentially to develop a powerful, practical algorithm for Quantum Molecular Dynamics applicable to large realistic systems, in particular of the HEDM type. Note that despite impressive progress, current "numerically exact" methods for quantum dynamics are confined to systems of a few modes only (Ref. 7). In the author's judgement, the project had important success in producing a time-dependent quantum simulation method that can treat large systems - a major leap compared with previous capabilities. The method was shown by tests to be of good accuracy, and is applicable to realistic, complicated interaction potentials. The novel method developed is not along the detailed lines envisaged in the original proposal. The Time-Dependent Self-Consistent Field (TDSCF) approximation (Ref. 8) and extensions thereof is used, as a basis for the Quantum Molecular Dynamics algorithm. Although interesting results were obtained here with the TDSCF method in this project, and although in special "niches" it was shown to provide a very useful approach, it cannot serve as the "method of choice" for this purpose: The TDSCF and especially its extensions, proved computationally too costly. The new method, developed in the present project, is based on the Classical Separable Potential (CSP) approximation, but includes also extensions of high accuracy, that are nevertheless computationally feasible. The CSP method was reported in a series of articles (Refs. 2-4), though the latest and most powerful extensions

are yet to be published. The essential idea in the CSP is to use a classical Molecular Dynamics simulation for the process of interest, to help "guide" the quantum simulation, and simplify the latter. This is done by using the classical MD to generate dynamical mean potentials for each degree of freedom. The mean potentials are then used in quantum calculations to generate a set of "orbitals" for each degree of freedom - orbitals for the motions of atomic coordinates. The time-dependent multi-dimensional wavefunction of the full system is constructed from the "orbitals" mentioned. The SCP was tested and developed first for systems of moderate quantum effects, e.g., cryogenic heavy atom systems. However, the use of classical MD only for the limited purpose of constructing effective potentials also seems to cause no difficulties in applications in solid hydrogen systems. In the following subsection the general principles of the method are described, with applications to cryogenic systems of semiclassical behavior ($\text{Ba}(\text{Ar})_n$ clusters). Applications to Mg in solid hydrogen, both partly completed, will be discussed in a later section.

2.1.2 The CSP Method and its Extensions: First is described the method for adiabatic systems. The method was outlined in (Refs. 2-4), and is based on the Classical Separable Potential (CSP) approximation. As a first step preceeding the quantum calculation, a full classical MD simulation of the same process was carried out. Let $V(q_1, \dots, q_N)$ be the full potential function of the system, and let $q_1^{(\alpha)}(t), \dots, q_N^{(\alpha)}(t)$ be the trajectory corresponding to the α initial conditions. For each mode q_i , an effective potential for that mode is defined:

$$\bar{V}_i(q_i, t) = \sum_{\alpha=1}^n V(q_1^{(\alpha)}(t), \dots, q_{i-1}^{(\alpha)}(t), q_i^{(\alpha)}(t), \dots, q_N^{(\alpha)}(t)) w^{(\alpha)} - \bar{V}(t) \quad (1)$$

The coordinate-independent quantity $\bar{V}(t)$ is chosen for convenience so that the mean value over the trajectories of the sum of the single-mode potentials at time t equals the value of the full potential of the system at that time. $w^{(\alpha)}$ in Equation (1) is the weight of the α initial condition, and n is the number of trajectories used. The single-mode effective potentials are used to generate single-mode wavefunctions, or time-dependent "nuclear orbitals", by solving the time-dependent Schrödinger equation:

$$i\hbar \frac{\partial \phi_j(q_j, t)}{\partial t} = [T_j + \bar{V}_j(q_j, t)] \phi_j(q_j, t) \quad (2)$$

where T_j is the kinetic energy of mode j . A first, but often very useful approximation for the total wavefunction in terms of the "nuclear orbitals" is given by the product:

$$\psi(q_1, \dots, q_N, t) = \prod_j \phi_j(q_j, t) \quad (3)$$

This approximation is similar in some respects to the TDSCF approximation (Ref. 8) and has about the same accuracy - but is incomparably more efficient for large systems. It is readily applicable to large polyatomics and to condensed phases. The great computational simplicity of the method, and of obtaining the "nuclear orbitals", together with other ideas, makes it feasible to proceed to much higher-level approximations, using a sum of terms of the product type Equation (3):

$$\Psi(q_1, \dots, q_N, t) = \sum_k C_k(t) \prod_{j=1}^N \phi_j^{(k)}(q_j, t) \quad (4)$$

With a sufficient number of terms, this "Configuration Interaction" expansion in terms of the time-dependent nuclear orbitals can be exact in principle. As practically applicable, it can provide an excellent approximation even for large systems. The equations of motion for the $C_k(t)$ are obtained by substitution of Equation (4) into the time-dependent Schrödinger equation.

The basis for the great efficiency of the CSP is in the very efficient production of the time-dependent orbitals for atomic motions, which in turn is due to the use of classical MD to construct the single-mode effective potentials, from which the orbitals are obtained. This is vastly superior to the effort required in TDSCF, where effective potentials are obtained in a quantum mechanical self-consistent procedure, involving computationally costly integrations. The classical MD calculation can be effective also in suggesting which of the enormous number of possible configurations in Equation (4) should be retained. We do not give the details here, but a quantity that plays a key role is the "correlation potential"

$$\Delta V(q_1, \dots, q_N, t) = V(q_1, \dots, q_N) - \sum_i \bar{V}_i(q_i, t) \quad (5)$$

where V is the full potential of the system, and the $\bar{V}_i(q_i, t)$ are the CSP single-mode effective potentials. ΔV represents the dynamical correlation between the various degrees of freedom, not present in the simple CSP. A set of orbitals of Equation (4) that provides a sufficient basis to represent ΔV is enough for an accurate solution of the Schrödinger equation. Calculations in the "Configuration Interaction" extension of CSP can practically include several hundreds of terms in Equation (4), and this is by the evidence of numerical tests, sufficient for quite good accuracy even in large systems.

For some processes and systems, especially when the required time scales are very short (say, $t \ll 1000$ femtoseconds), the simplest level of CSP suffices. However, for processes involving nonadiabatic transitions between different electronic states, this is never the case. The method then requires important generalizations:

(i) Rather than use classical MD, one determines trajectories from a semiclassical MD that allows for transitions between different electronic states. We used for this purpose Tully's semiclassical surface-hopping method.(Ref. 9) From these trajectories one can construct effective single-mode Hamiltonians, and use the latter to construct the time-dependent single-mode orbitals.

(ii) The effective Hamiltonians constructed in this case already include the effects of nonadiabatic transitions. The full approach requires in this case the use of a wavefunction that has at least n terms, each of which is a simple product of orbitals (single-mode wavepackets), n being the number of electronic states involved. The form of the wavefunction in the nonadiabatic case is, in the simplest version:

$$\Psi(\mathbf{r}, q_1, \dots, q_N, t) = \sum_{k=1}^n C_k(t) \psi_k(\mathbf{r}, \mathbf{q}) \chi^{(k)}(\mathbf{q}, t) \quad (6)$$

where

$$\chi^{(k)}(\mathbf{q}, t) = \prod_{j=1}^N \phi_j^{(k)}(q_j, t) \quad (7)$$

In Equation (6), \mathbf{r} denotes the electronic coordinates and \mathbf{q} the nuclear ones. The $C_k(t)$

are time dependent coefficients, and are determined by solution of the Schrödinger equation. The orbitals $\phi_j^{(k)}(q_j, t)$ are determined by solving the time-dependent equation for the effective Hamiltonians associated with the individual modes q_j . The full procedure in the nonadiabatic case is described in Ref. 4. Tests for small model systems have shown that this is an approach of very good accuracy.

2.1.3 Applications: The CSP method and its extensions were tested extensively for small model systems, and were applied already to several realistic cases, all in the framework of the present project. The earliest tests of the simple SCP were for photoinduced processes in collinear model clusters, e.g. photodetachment dynamics of $\Gamma(\text{Ar})_2$, and photodissociation of HX in $\text{Rg} \cdots \text{HX}$. (Ref. 2) Many of the more recent tests are also for triatomic systems, since for such small systems there are exact reference calculations by other time-dependent methods. Estimates of the errors involved can be carried out in the framework of the method itself (based on calculations of correction terms), and these were used for some of the realistic applications.

The first applications to realistic systems were for processes in cryogenic clusters of Ne and Ar atoms, rather than for hydrogen systems. The less pronounced nature of the quantum effects in the "semiclassical" clusters made applications and interpretations with the new method simpler, since the physics of the processes involved is easier to understand. Discussed here is such an application to a heavy-atom cryogenic cluster, and defer to Section (2.8) results on simulations for Mg in H_2 clusters, which is a system of direct HEDM relevance. The application described here is of the photoexcitation dynamics of $\text{Ba}(\text{Ar})_n$ clusters, with $10 \leq n \leq 20$. A major reason for choosing this system is that one expects it to be, at least to some extent, a useful (if more classical) model for $\text{Mg}(\text{H}_2)_n$. Another important reason is that interaction potentials of good quality were available in this case from empirical sources. (Ref. 10) Finally, for large $\text{Ba}(\text{Ar})_n$ clusters, experimental results were available from the group of Mestdagh, Visticot *et al.* (Refs. 10,11) in Saclay, France. In fact, in a recent joint study with that group, a nearly quantitative interpretation for their findings was provided. (10)

The application is described in detail in a paper by Jungwirth and Gerber. (Ref. 4) Using the new method described above, the $\text{Ba}(\text{S}) \rightarrow \text{Ba}(\text{P})$ excitation in $\text{Ba}(\text{Ar})_n$ clusters, for $n = 10, 20$ was simulated. The structure of the clusters in the electronic ground state roughly corresponds to a Ba atom adsorbed on a surface of Ar atoms. For this structure the 3 excited P -type singlet state can be classified as one Σ -type state (where the orientation of the p -orbital of the Ba is roughly normal to the surface) and two Π -type states (where the p -orbital density is approximately parallel to the surface). In the dynamical calculations excitation into the highest (Σ -type) state was considered, and followed the development of the system in time. The CSP results were compared with those of semiclassical surface hopping calculations (Tully's method). The nonadiabatic version of the CSP, with 3 configurations in the wavefunction expansion (Equation (6)) was used. Tests indicate that the CSP results are very accurate in this case, and the validity of the method holds for times up to $t \approx 1.5$ fs and probably longer. Some of the main results are shown in Figs. (1), (2). To emphasize some of the key points:

(i) The very symmetric, well-defined structure of the initial state is destroyed by the excited state motions within a timescale of $t < 500$ fs. As Figure 1 for the $\text{Ba}(\text{Ar})_{10}$ shows, the initial state corresponds to 3 very narrow peaks in the Ba-Ar distance

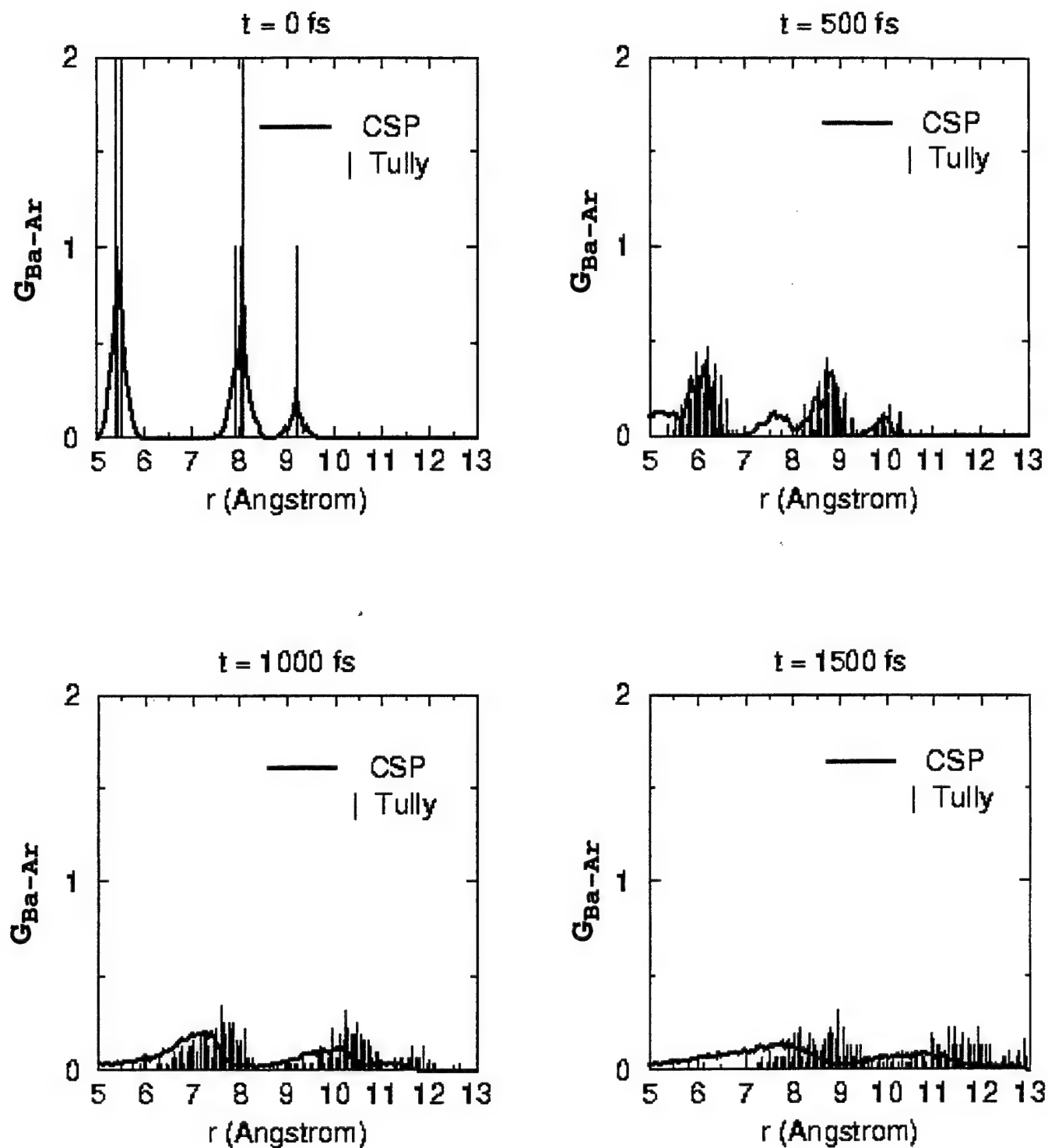


Figure 1
Time Evolution of the Ba-Ar Atom-Atom Distribution Function for the $\text{Ba}(\text{Ar})_{10}$ Cluster

distribution, reflecting a well-defined relatively rigid cluster structure where the Ba is adsorbed on top of an approximately planar (Ar)₁₀. The 3 main Ba-Ar distances are only faintly recognizable at $t = 500$ fs, and the whole structural distribution has become smeared. The trend continues for longer times excitation, and for $t = 1500$ fs the distribution is so broad and smeared that it is meaningless to attribute a structure to the cluster. Most of the smearing is due to the motion of the Ba atom away from the (Ar)₁₀ surface (the probability for direct dissociation of the cluster in this process is about 80%), but there are also changes in the structure of the (Ar)₁₀ "surface".

(2) Figure 2 shows the relative populations (branching ratios) of the three different electronic P -states of the Ba(Ar)₁₀ system, as a function of time. The figure shows that electronic relaxation from the Σ to the Π states becomes significant after a timescale of ~ 1 picosecond or less, the released energy going, of course, into the vibrational degrees of freedom of the cluster. The relaxation is dominantly into the state intermediate in energy - the population of the lowest Π state remains extremely small at least through the first 1500 fs of the process.

(3) For Ba(Ar)₁₀, direct dissociation is the dominant process ($\sim 80\%$). Only about 20% of the wavepackets describe electronic relaxation into the Π state and stabilization of the cluster. In the case of Ba(Ar)₂₀, electronic relaxation greatly dominates over direct dissociation. (Direct dissociation is about 20% only). This trend becomes stronger for larger Ba(Ar) _{n} clusters: For the experimental clusters of Visticot *et al.* (Refs. 10,11), with $n \gg 100$, our simulations showed that evaporation of Ba from the cluster after excitation is a fairly rare event, with a probability of several percent at most. (Ref. 12) As cluster size increases, so does the binding energy, and therefore the decrease of direct dissociation. Electronic relaxation becomes slower also with cluster size, but less so than direct dissociation. It has a timescale of 10^3 fs only for the very large clusters. These conclusions on electronic relaxation of excited metals in cryogenic media are of importance for HEDM purposes, since electronic excitation has been used to characterize and study metal-doped solid hydrogen systems. (Refs. 13,14)

(4) Figure 2 shows that the semiclassical surface-hopping method can be in significant error in predicting electronic branching ratios. Qualitatively, the prediction of this method of the populations in time looks reasonable, but the result for the population of the intermediate level is off by a factor of 2 for $t = 1.5$ fs. (The error for the lowest state is even greater, due to the fact that one deals with a very low population there, the magnitude of which is hard to get accurately). On the other hand, the semiclassical method is successful in predicting quite reasonably the change of the structure of the cluster in time - see Figure 1. Thus, even for heavy atom clusters, the semiclassical surface hopping method must be used with caution, and only for certain properties. Whenever possible in doubtful cases, use of the new method proposed here is recommended.

2.1.4 State of the Method and Future Directions: The algorithm and code for the simplest level CSP have already been developed to a level of an efficient, user-friendly tool. Simulations for several systems with over 150 coupled degrees of freedom have been carried out. Code development, with emphasis on implementation on parallel computers, continues. Anticipated are applications for systems with over 500 atoms (1500 degrees of freedom) in a matter of months at most. When simple CSP suffices, it is already a very powerful practical tool for Quantum Molecular Dynamics. The extension of the method

quantum (CSP)

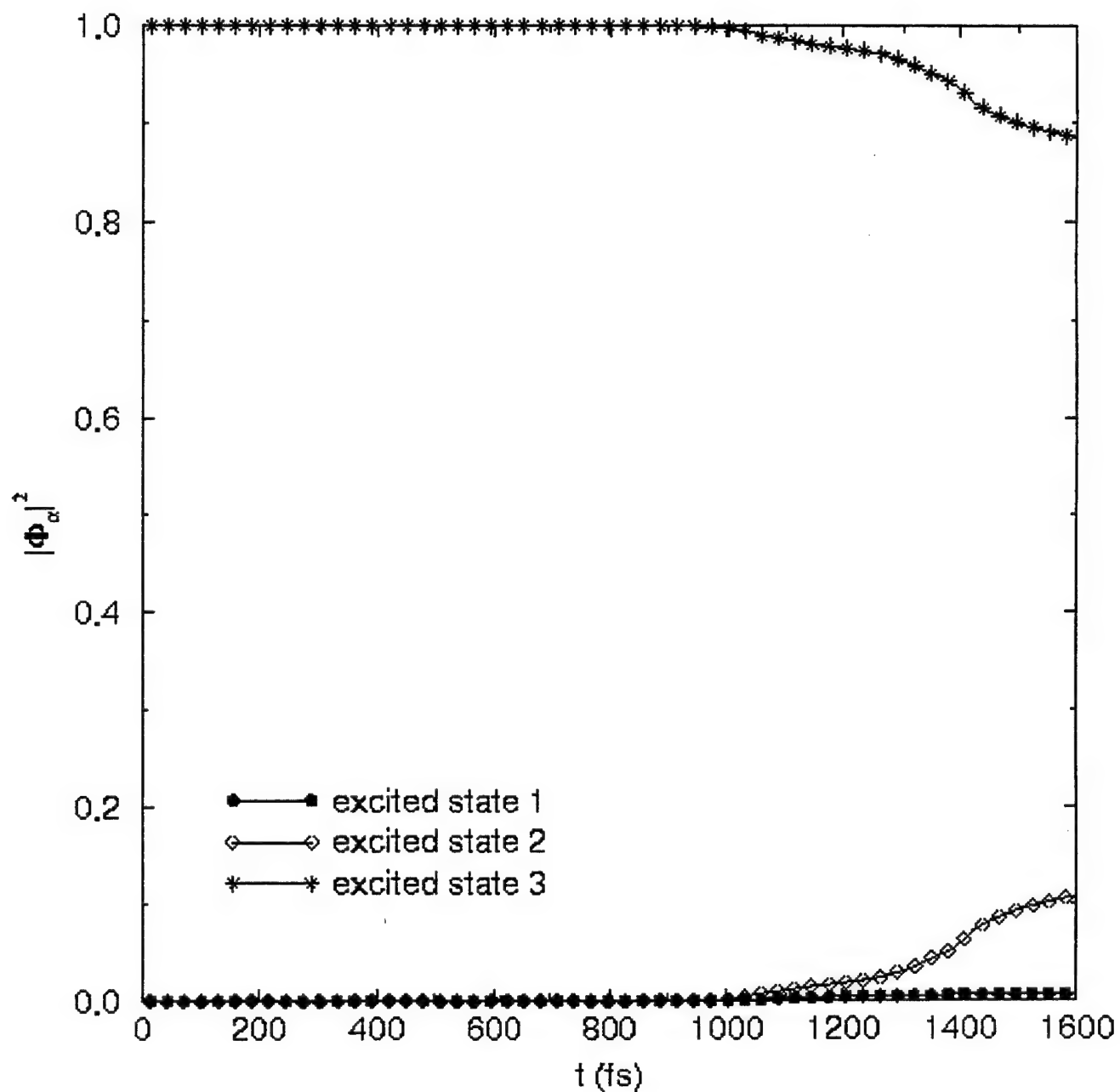


Figure 2a
Branching Ratios for the S-Type and the Two P-Type Excited States of the $\text{Ba}(\text{Ar})_{10}$ Cluster

semiclassical (Tully)

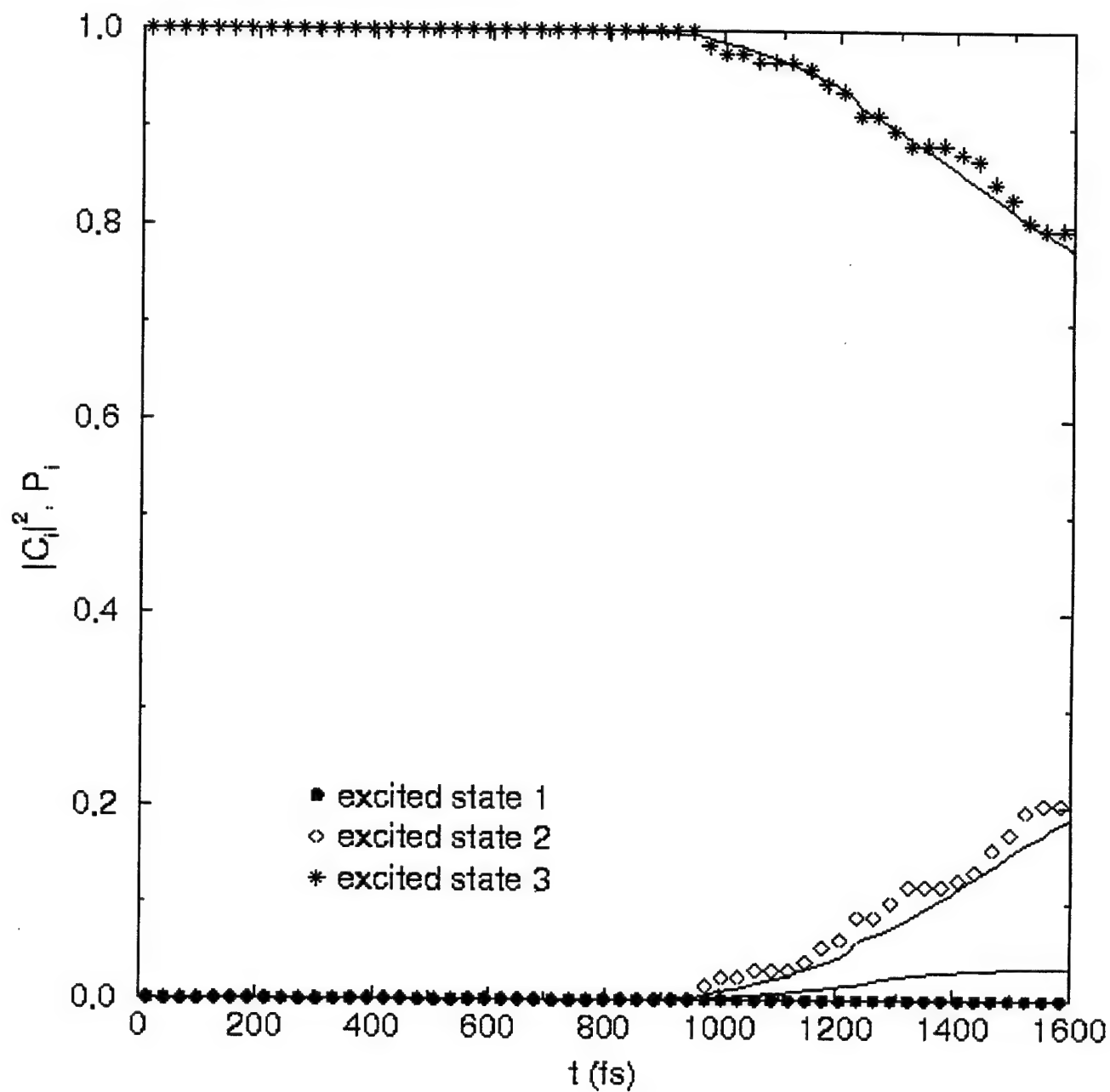


Figure 2b
Branching Ratios for the S-Type and the Two P-Type Excited States of the $\text{Ba}(\text{Ar})_{10}$ Cluster

to include many configurations, as in Equation (4), has the advantage of making the approach very accurate (in fact, with a sufficient number of terms in Equation (4), it should be "numerically exact"). The practical performance in accuracy of the method, in all test cases, is very promising and exciting. However, the largest calculations with it are still confined to ~ 15 atoms (less than 50 degrees of freedom). Again, developments on this are very fast, and systems of the order of a few hundreds of modes should be developed within a year or so. Presently, there is no other method of similar accuracy for the system sizes treated.

2.2 Quantum and Semiclassical TDSCF Simulations of Cryogenic Systems

The original plan for this research was to develop a time-dependent quantum method for simulations of many-particle systems based on the Time-Dependent Self-Consistent Field (TDSCF) approximation. (Ref. 8) A CSP was developed as the simulation tool for the purposes of this project, and as a powerful and practical algorithm for time-dependent quantum simulations of large systems in general. Nevertheless, much of the research on this project dealt with TDSCF, and some very useful results were obtained with this method. As seen below, the method is useful in some practical applications, including certain specific systems of HEDM interest, although in general it does not seem to compete favorably with CSP. Presented now are the TDSCF results obtained in the project, with some comments and conclusions on HEDM applicability. The TDSCF approximation has been known in general formulation from the early stages of quantum theory, and has been in extensive use by several groups, including the author's group. This refers to a review by Ratner and Gerber on the principles of the method. (Ref. 8) Examined here are conclusions and findings obtained in this project.

As seen below, simulations have shown that TDSCF is of good accuracy for very short timescale dynamics ($t \ll 1000$ fs) even for hydrogen clusters. (Ref. 15) For longer times, extensions are required if accuracy of the description is to be maintained. The TDSCF, as the simplest version of the CSP, represents the total wavefunction of the system as a product of time-dependent single-mode wavepackets (nuclear orbitals). Extensions of TDSCF have been proposed that require sums of terms in the wavefunction expression with each term being a product of single-mode wavepackets (Refs. 16-20), such as multiconfiguration TDSCF. (Refs. 18-20) The failure of TDSCF is only a failure of computational efficiency:

(1) For large systems and for complicated interaction potentials, the TDSCF approximation itself becomes computationally very costly. The calculation of single-mode effective potentials involves, for realistic interactions between the particles, the evaluation at each time point of multidimensional integrals. As a result, even for systems with a modest number of modes, say ~ 10 , the CSP is by an order of magnitude computationally superior to TDSCF.

(2) In the multiconfiguration version of the theories, the handicap of TDSCF is even more severe. Multiconfiguration TDSCF is a very accurate high level algorithm for molecular dynamics, and works very well also for HEDM-type systems, but is essentially limited to systems of several atoms (except if one has the advantage of very special, simple potentials which are usually unrealistic) CSP has an enormous advantage in the efficiency of generating the single-mode wavepackets, and also in assessing how many and which types of configurations should be included (these are due to the use of classical MD in

generating effective one-mode potentials, hence orbitals, and in providing guidance for the quantum calculation.) TDSCF becomes thus a practical method either for simple systems, or when special simplifying potentials can be used.

Validity of the TDSCF approximation for the dynamics of hydrogen clusters: In order to test whether TDSCF holds for the dynamics of HEDM-type materials, we carried out comparisons between TDSCF and exact calculations for small metal atom - hydrogen clusters. (Ref. 15) One of the systems for which the calculations were done is a collinear model of the cluster $B(H_2)_2$, having the structure $H_2 - B - H_2$. For such a small system, numerically exact solutions of the time-dependent Schrödinger equation is possible. The TDSCF approximation, the accuracy of which depends on the choice of coordinates since the approximations involve a mutual separation of the modes, was applied in normal coordinates. In the calculations, a non-stationary, but bound, initial state of the cluster $\Psi(q_1, q_2, t=0)$ was propagated in time exactly, and also in the TDSCF approximation. The autocorrelation function of the wavefunction $\langle \Psi(q_1, q_2, t) | \Psi(q_1, q_2, 0) \rangle$ was one of the quantities used to compare the TDSCF and the exact results. This is a phase-sensitive quantity, and quite demanding for the approximation. It was found that the TDSCF approximation remains valid within reasonable accuracy to times of the order of $t \leq 50$ fs for $B(H_2)_2$. In this domain, the autocorrelation function computed from TDSCF is accurate to 80% or better. For longer times, the TDSCF approximation error builds up, and application will therefore require extensions of TDSCF, as discussed above. These calculations of Li and Gerber thus show that the TDSCF is applicable for HEDM-type systems, in ultrafast time domains. As mentioned earlier, the problem in applying the TDSCF is the computational effort that is involved for large, real systems. TDSCF calculations are feasible and efficient for large collinear model clusters, and such calculations were carried out by Li and Gerber for $(Ne)_n$, $n \leq 16$. (Ref. 21) For large clusters in 3D geometry, the calculations became very costly, and TDSCF is computationally much inferior to CSP, except when certain specific, advantageous potential functions can be used, as discussed below.

TDSCF simulations for large systems with quartic force fields: In cases when the multidimensional potential surface can be expanded as a power series in the coordinates with a sufficiently low maximal power, the TDSCF was found to be practically applicable and efficient, and can be used for Quantum Molecular Dynamics simulations of large systems in 3D geometry. It was discovered that for the clusters $(Ar)_{13}$ and $(Ne)_{13}$ for instance, a quartic representation of the potential in the normal modes is of sufficient accuracy with low energies.(20) Thus, a potential function of the form:

$$V(q_1, \dots, q_N) = \sum_{n(i) \geq 0} C_{n(1), \dots, n(N)} (q_1)^{n(1)} \dots (q_N)^{n(N)} \quad (8)$$

was used where the $C_{n(1), \dots, n(N)}$ are the expansion coefficients, and $n(1) + \dots + n(N) \leq 4$. Using this force field, simulations of $(Ar)_{13}$, $(Ne)_{13}$ were carried out and other large clusters in full 3D geometry. (Ref. 22) There were semiclassical TDSCF simulations, where in addition to the TDSCF approximation, a semiclassical Gaussian approximation is used for the single mode wavepackets. The semiclassical approximation holds in cases when the anharmonicity is not very large. To test the method for a large, realistic system equilibrium simulations were carried out, that is, the semiclassical TDSCF for, e.g., $(Ar)_{13}$, $(Ne)_{13}$ was run until the system reached equilibrium, for which criteria was provided. (Ref. 22) The results were compared with the

Feynman Path Integral (FPI) simulations which was carried out for the same system: The FPI is "numerically exact", but cannot be used in practice for real-time simulations, only for equilibrium ones (for realistic cases). The FPI could be used to test the semiclassical TDSCF. Figure 3 shows a comparison between the radial distribution function $g(r)$ computed from TDSCF, and the corresponding result from FPI, (20) for $(\text{Ne})_{13}$. Both calculations are for $T = 2\text{K}$. The agreement is excellent, establishing the validity of semiclassical TDSCF for this system. For hydrogen clusters and solids under normal conditions, the anharmonicity is so high that expansion (Equation (8)) takes many terms to converge, and the approach is impractical. However, for hydrogen at high pressure, $P \geq 5\text{kbar}$, say, the anharmonicity is no longer so severe, and expansion (8) can be used with a reasonable number of terms. Thus, it is shown that TDSCF can be applied for time-dependent quantum simulations of solid hydrogen and doped hydrogen materials at high pressure. The method can also be applied to other cryogenic systems, like solid Ne, that are not of HEDM applications but are useful as models in HEDM research. In conclusion, it is shown that the TDSCF method can be useful as a Quantum Molecular Dynamics simulation tool in HEDM research, but only for a restricted class of systems.

2.3 Algorithms for Equilibrium Simulations of Quantum Clusters

The tasks set at the initiation of this research project also required simulations of ground-states or thermal equilibrium states of HEDM-related systems. For instance, calculations of time-dependent dynamical processes in the systems of interest often require simulations of equilibrium states as the appropriate initial states for the dynamical processes. Essentially, the photoinduced processes considered in this work begin from an equilibrium system. Simulations for two types of equilibrium states were carried out: (1) The vibrational ground state of HEDM-related clusters or solids; (2) Thermal equilibrium states at finite temperature of these systems. For both types of calculations methods well-established in the literature were used, but developed in each case its own specific algorithms and codes, which have specific advantages for our purposes compared with other, exciting ones based on the same basic methods. The simulations using these codes played a major role in accomplishing the tasks as set in projects detailed in the Program Plan. In addition, the availability of the codes may prove a useful future resource for HEDM research by other groups.

2.3.1 Diffusion Quantum Monte Carlo (DQMC) Simulations of Vibrational Ground States of HEDM Systems:

DQMC, and related methods such as Variational Quantum Monte Carlo, are amongst the powerful available techniques for calculations of the ground state of large quantum systems. (Refs. 23-28) Our work (in cooperation with M. Alexander) was the first to extend the method for systems containing an open-shell, p -state atoms. (Ref. 29) Also, a code was developed for implementing the work on a massively-parallelized computer (Ref. 30) and indeed the work was mostly carried out on the MasPar2 at U.C. Irvine, a system of 4096 nodes. This resulted in a capability to simulate large systems very efficiently. In the simulations described in the forthcoming sections DQMC was used to obtain structural and energetic properties of potential HEDM systems. Table 1 presents data on the energies of HEDM-related clusters obtained in our calculations, and more extensive data and analysis of the main systems is presented later on in this report.

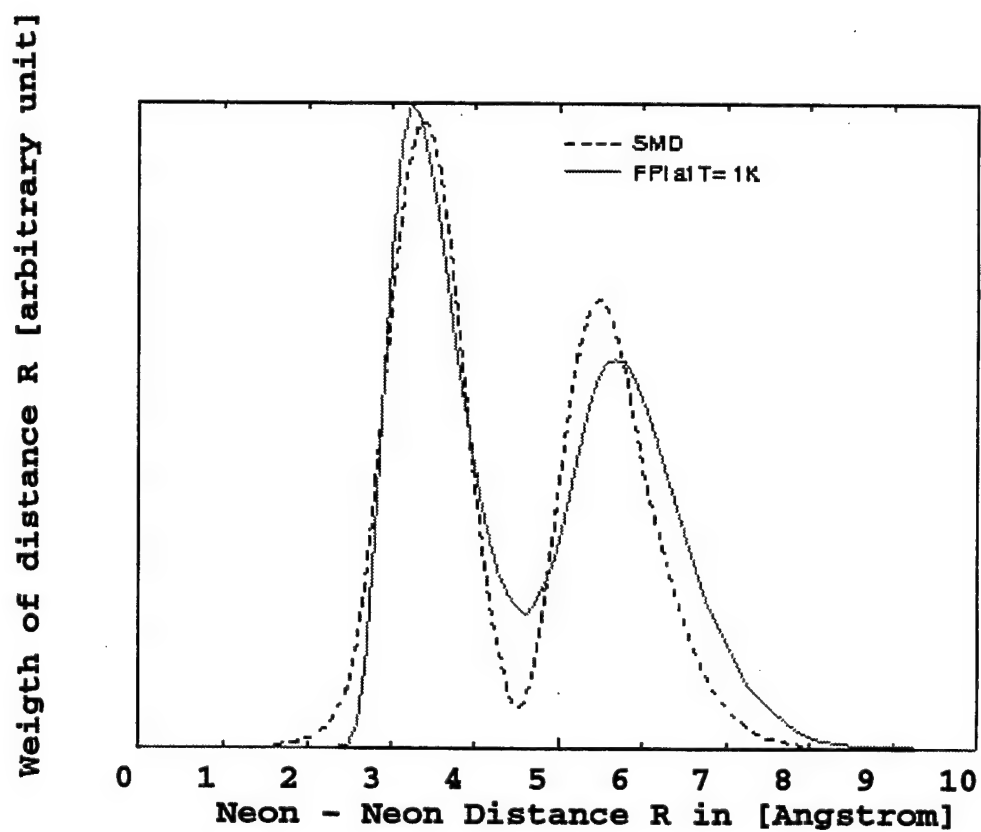


Figure 3
The Ne-Ne Distance Distribution function for $(\text{Ne})_{13}$ at $T=1\text{K}$. Semiclassical Molecular Dynamics Results are Compared with Feynman Path Integral Simulations.
From Ref. (22)

Table 1. DQMC Results for the Cohesion Energy of Quantum Clusters

Cluster	Vibrational Energy $D_0(\text{cm}^{-1})$
$\text{H}_2 - \text{H}_2$	1.86
$(\text{H}_2)_3$	6.867
$(\text{H}_2)_4$	14.06
$(\text{H}_2)_5$	25.01
$(\text{H}_2)_6$	34.65
$(\text{H}_2)_{10}$	86.99
$(\text{H}_2)_{13}$	134.5
$(\text{H}_2)_{45}$	515.54
$(\text{H}_2)_{100}$	843.02
$\text{Hg} - \text{H}_2$	13.65
$\text{Hg} - (\text{H}_2)_2$	31.80
$\text{Hg} - (\text{H}_2)_{10}$	212.3
$\text{Hg} - (\text{H}_2)_{12}$	282.8
$\text{Hg} - (\text{H}_2)_{24}$	485.0
$\text{Hg} - (\text{H}_2)_{40}$	687.7
$(\text{D}_2)_3$	16.0
$\text{Li} - \text{H}_2$	8.5
$\text{Li} - (\text{H}_2)_2$	3.6
$\text{O} - \text{H}_2$	15.00
$\text{O} - \text{D}_2$	19.80
$\text{F} - \text{H}_2$	14.06
$(\text{Ar})_{13}$	4586.8

2.3.2 Feynman Path Integral Simulations of Quantum Systems at Thermal Equilibrium: Extensive work on this topic was done for $\text{Li}(\text{H}_2)_n$ clusters by Klein and coworkers. (Ref. 31) The FPI simulations were applied to structural and energetic properties of $\text{Mg}(\text{H}_2)_n$ and other quantum clusters. (Ref. 32) The algorithm (Ref. 22) followed the approach of References (33) and (34). Also, the algorithm was recently extended for FPI simulations of systems containing open-shell atoms. Furthermore, the algorithm was implemented in codes for distributed computers. The FPI simulation data are given in subsequent sections.

2.4 Structural Properties, Stability and Dynamics of $\text{B}(\text{H}_2)_n$ Clusters

The results obtained in this part are amongst the most important ones of the research project, since they support the suggestion that boron in hydrogen may be one of most promising candidates for a HEDM propellant. Indeed, the results seem most encouraging. This work was done in cooperation with M. Alexander and his group. The $\text{B}-\text{H}_2$ interaction potential used was taken from the *ab initio* calculations of Alexander. (Ref. 35) The calculations were done by Diffusion Quantum Monte Carlo (DQMC), adapted to deal with a system that includes an open-shell P -state atom. An extensive account of the results is given in Reference (29), and only a brief summary of the findings is given here. The calculations of Reference (29) were for $\text{B}(\text{H}_2)_n$, with $1 \leq n \leq 8$. Calculations for clusters with a much larger number of H_2 molecules (up to $n = 100$) are under way. The preliminary results support the conclusions below, and are based on the small-cluster data. Listed below is a summary of the findings, and of the conclusions regarding structural properties, energetic stability, boron atom diffusivity and vibrational properties of boron-hydrogen clusters:

(1) $\text{B}(\text{H}_2)_n$ clusters are energetically very stable, compared with pure H_2 clusters or with clusters of S -state atoms (e.g., Li, Mg) with hydrogen molecules. As Table 2 shows, one expects $\text{B}(\text{H}_2)_n$ (at least for $n \leq 6$), to remain stable well above the melting point of pure solid hydrogen. The low energy of the minima of the potential functions are offset in part by the high zero-point energies. Nevertheless, on the basis of the results, B atoms in solid H_2 should undergo strong complexation with neighboring hydrogen molecules. At a temperature of 4K, considered in some HEDM designs, the solvated boron atom should be extremely stable.

(2) To further quantify the energetic stability of $\text{B}(\text{H}_2)_n$ clusters, and the effective solvation of boron by hydrogen, the accretion energy and the solvation energy of the $\text{B}(\text{H}_2)_n$ clusters was considered. The accretion energy is defined as the energy gained by adding one more H_2 molecule to $\text{B}(\text{H}_2)_n$. The solvation energy is defined as the energy gained by adding a B atom to a pure H_2 cluster. The accretion and solvation energies, as a function of cluster size, are shown in Figure 4. The special stability of the $n = 5$ cluster is evident from the results. The values of accretion and of solvation energy for all the clusters shown are very large on the scales of such quantities found for $\text{M}(\text{H}_2)_n$ clusters, where M is an alkali or an earth-alkali metal (Li and Mg were considered).

**Table 2. Calculated Potential Energy Minima
and Lowest Vibrational Energies of B(H₂)_n**

<i>n</i>	Potential Minimum	Vibrational Energy
1	-61.3	-25.4
2	-146.8	-47.5±1.0
3	-233.7	-74.8±2.5
4	-309.0	-97.4±1.9
5	-410.8	-137.9±3.5
6	-523.7	-156.4±4.3

(Energies are given in cm⁻¹)

(3) The B(H₂)_n clusters are very anisotropic in structure. This stems from the dependence of the boron-hydrogen interaction on the unpaired *p*-orbital of the B atom: The interaction is considerably deeper when the H₂-B axis is normal to the direction of the *p*-orbital (π -state in a pseudo-atom treatment of H₂). Therefore, for low *n*, the lowest energy structures of B(H₂)_n are planar, with the plane of the H₂ molecules normal to the *p*-orbital. It must be kept in mind, however, that the structure of none of the clusters is rigid, but rather fairly delocalized. The structures corresponding to minima of the potential surfaces are shown in Figure 5 for *n* = 5, 6, 8. In each case are shown the structure corresponding to the global minimum, and the structure corresponding to local low-lying minima. The B-atom is at the center of the cluster for the global minimum of B(H₂)₆, but not in the other cases. The structures corresponding to the local minima of the potential surface differ in some cases substantially from the global minimum structure. Not in all cases is this important since the vibrational wavefunctions are very delocalized, and can be spread over several minima. At least some of the local minima are, however, outside the delocalization range, and thus the existence of multiple structural "isomers" is an important property of B(H₂)_n. In conclusion, one important finding are the highly nonspherical, anisotropic structures of B(H₂)_n and another is the fact that above the lowest temperatures several different structures may be populated.

(4) Data on the zero-point quantum fluctuation of the structures of B(H₂)_n, is presented in Figure 6. The upper part shows the distribution of B atom distances from the center of the cluster. The middle part of Figure 6 shows the distribution of H₂ distances from the center. Finally, the lower part shows the angular distribution of H₂ molecules with respect to the direction of the unpaired *p*-orbital of the B. It is evident that: (a) The structural distributions, due to the zero-point quantum fluctuations are large (although the structures are less delocalized than for the corresponding pure (H₂)_n clusters); (b) The B atom is much closer to the center of the cluster than the H₂ atoms that "surround" it; (c) The zero-point motions are not sufficient to "smear out" the anisotropic structure of the B(H₂)_n clusters.

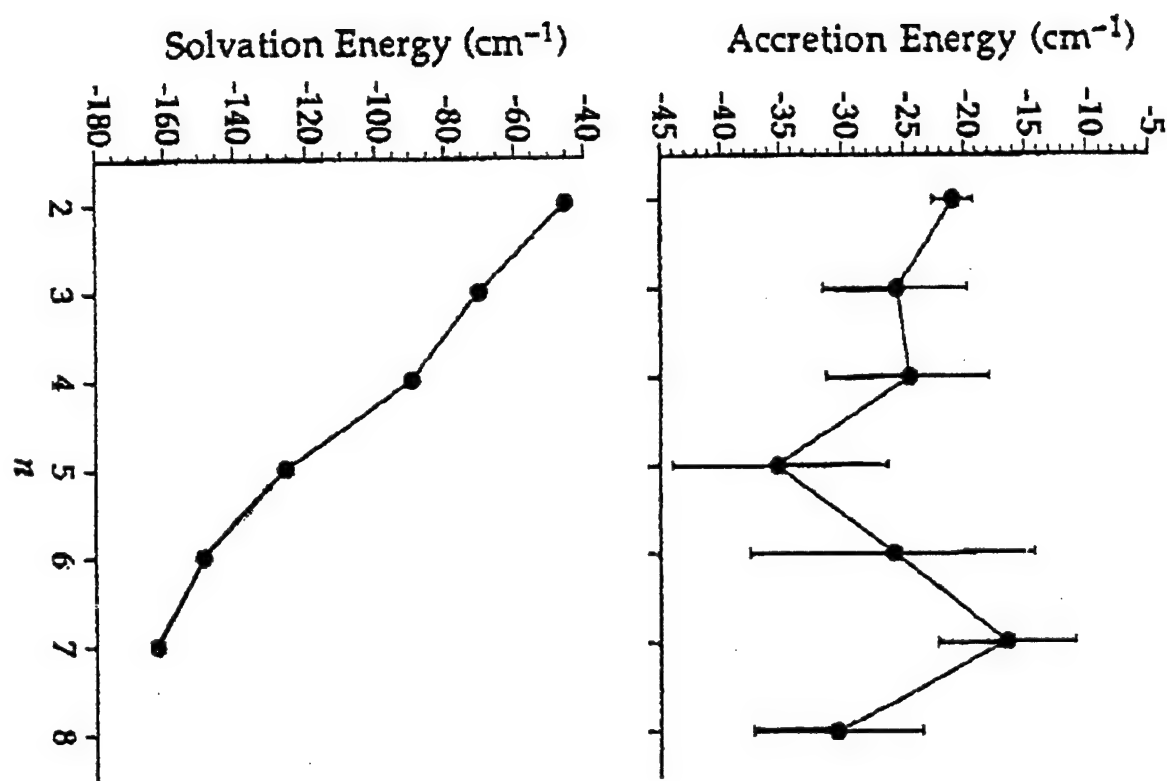


Figure 4
The Accretion Energies (Right Panel) and Solvation Energies (Left Panel) of $B(H_2)_n$ as a Function of n

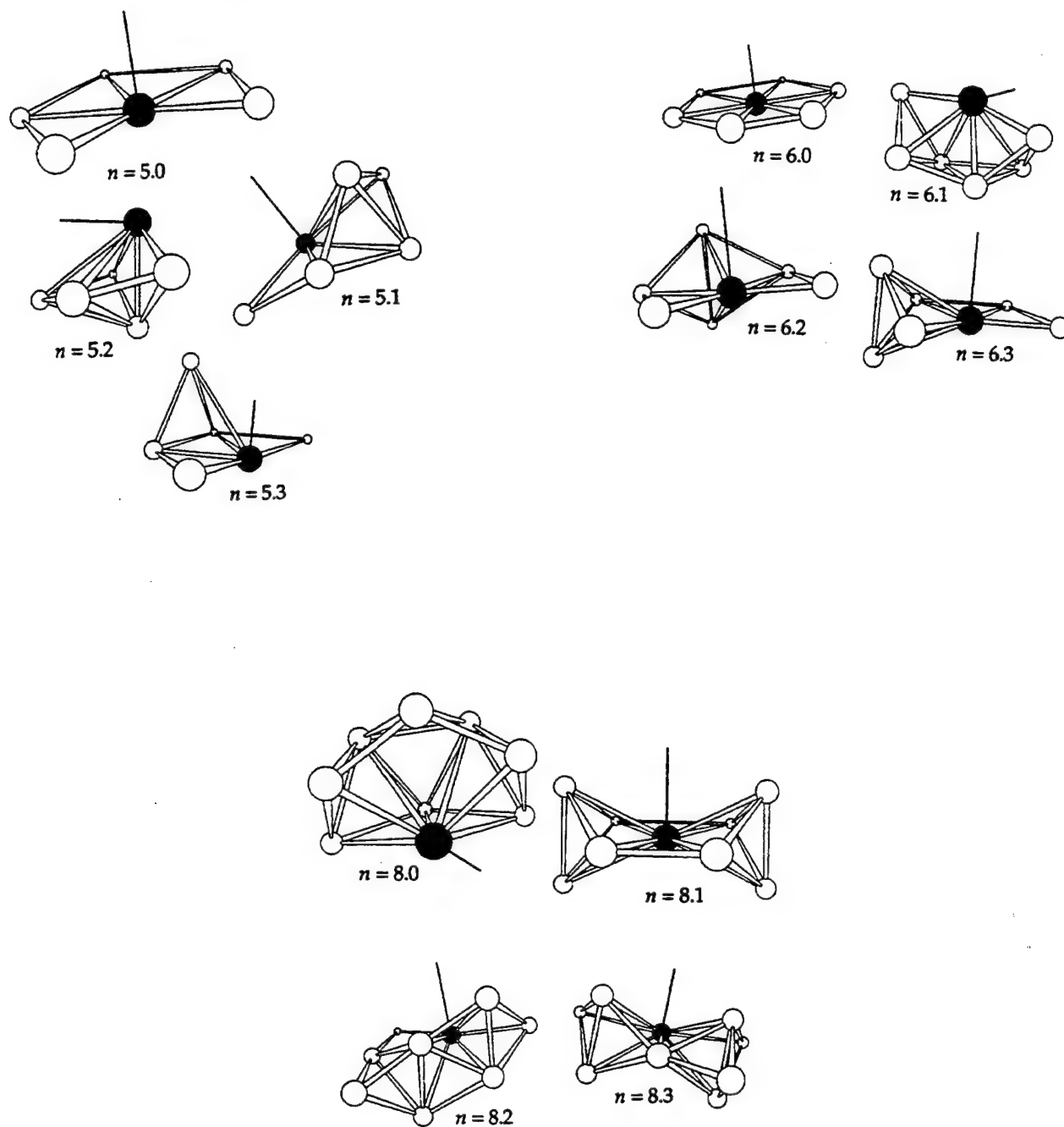


Figure 5
 The Structures of Global and Local Minima of Clusters $B(H_2)_n$. The Notation $n.m$ is Used to Designate Minimum m of the Cluster with n Hydrogens. $m = 0$ is the Global Minimum, $m = 1$ is the Lowest Local Minimum, etc.

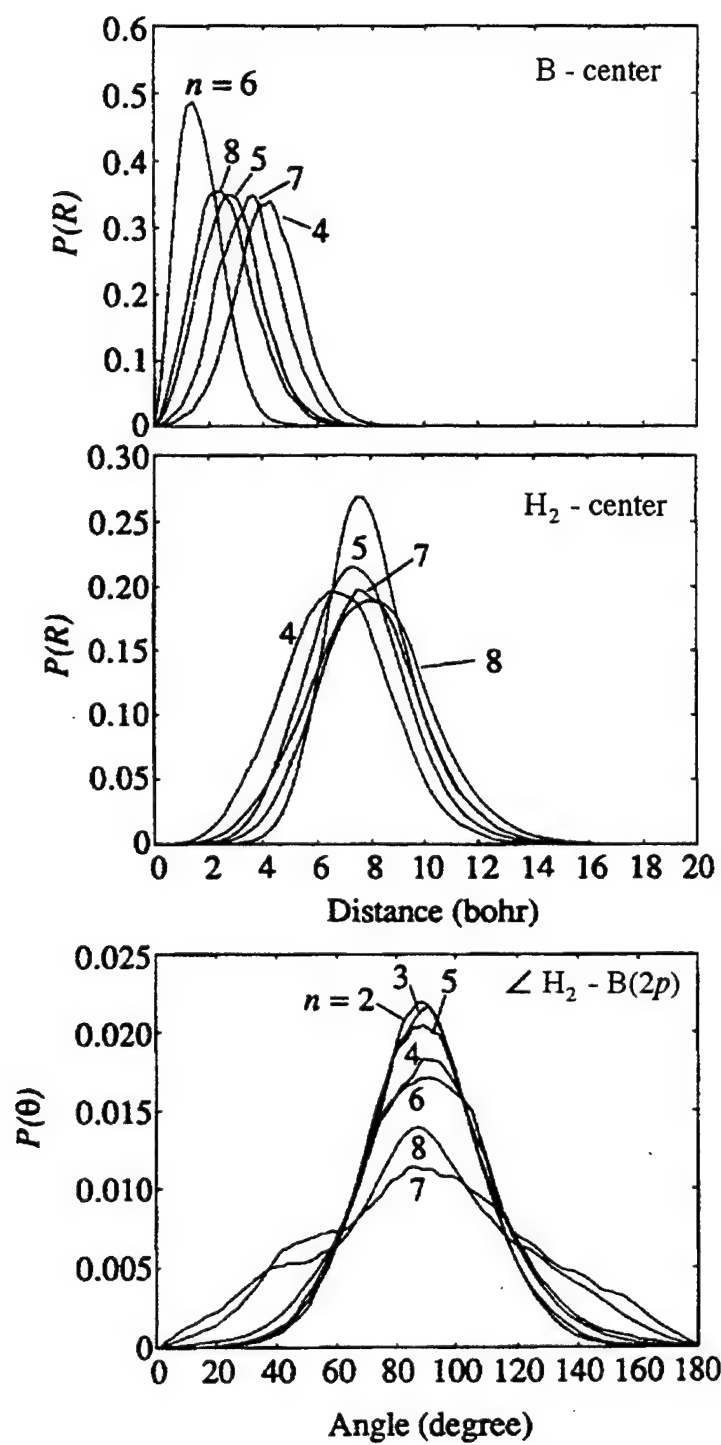


Figure 6
Structural Distribution for $B(H_2)_n$ from DQMC

(5) The role and extent of H_2 orientation within the clusters were determined in the case of $B(H_2)$. While in $B(H_2)$ there is more anisotropy of the H_2 orientation than, e.g., in $(H_2)_n$, or in $Li(H_2)_n$, the anisotropy is slight, and one can treat the H_2 as a spherical particle to good approximation.

(6) From the strong binding of the small clusters $B(H_2)_n$, it is inferred that diffusivity of B atoms in solid H_2 will be extremely low, up to the melting point of H_2 : The stable local $B(H_2)_n$ complexes in B-doped solid hydrogen will prevent diffusion of the boron. This implies that solid hydrogen doped with B should be stable against diffusion, and remain non-segregated, preferably up to the melting temperature of hydrogen. This is an important, favorable property of B in solid hydrogen for HEDM purposes. This part of the project accomplished Tasks 1 and 4 of the Program Plan of the research proposal.

2.5 Structural Properties, Stability and Vibrational Dynamics of $Mg(H_2)_n$ and Related Clusters

The calculations on $Mg(H_2)_n$ clusters were motivated by the estimates of P. Carrick of the Phillips Laboratory, suggesting that Mg in solid hydrogen has a high Specific Impulse, and should be of potential interest as a HEDM propellant. The objective of the calculations we carried out was to determine the energetic stability, the structural properties and the vibrational properties of $Mg(H_2)_n$. Calculations on the structural and energetic properties of metal-hydrogen systems were previously carried out by M. Klein and coworkers for $Li(H_2)_n$ and also for Li in solid hydrogen. (Refs. 31,36) These calculations, using the Feynman Path Integral method for thermal equilibrium simulations showed that in $Li(H_2)_n$ the Li is very weakly adsorbed on the surface of an essentially spherical $(H_2)_n$. An elegant experimental approach has made it possible for Fajardo and coworkers to "implant" Li impurities in solid hydrogen and study their spectroscopy. (Refs. 13,14) Nevertheless, the results of Klein and coworkers suggest very unfavorable prospects for preparing appreciable concentrations of isolated Li atoms in solid hydrogen. Prior to obtaining an interaction potential for $Mg-H_2$, (Ref. 37) simulations were carried out for $Hg(H_2)_n$, and is expected to prove similar in properties to $Mg(H_2)_n$. Although $Hg(H_2)_n$ is not a HEDM candidate, its properties are useful in throwing light on the expected behavior of $Mg(H_2)_n$.

(1) $Mg-H_2$ Interaction: In our DQMC simulations on $Mg(H_2)_n$, the $Mg-H_2$ potential was used, obtained by Jung and Gerber by SCF/MP-4 *ab initio* electronic structure calculations. (Ref. 37) Later, Chaban and Gordon provided their results for the same systems. (Ref. 38) The two potentials, computed by different methods, are quite similar. The $Mg-H_2$ potential has a slightly deeper well-depth than the H_2-H_2 interaction. The anisotropy of the $Mg-H_2$ potential at equilibrium distance is very weak (weaker than that for $B-H_2$, mentioned in the previous section), and can safely be ignored in simulations of $Mg-(para)H_2$.

(2) Ground-state structures of $Hg(H_2)_{12}$, $Mg(H_2)_{12}$: Figure 7 shows the $Hg-H_2$ in the vibrational ground state of the latter. (Ref. 30) Figure 8 shows the H_2-H_2 distance distribution for the same system. (Ref. 30) Analysis of these results and of other data from the DQMC calculations shows that the structure corresponds to Hg being inside a solvation shell of the H_2 molecules. (Ref. 30) The solvation shell is nearly spherical. Figure 9 shows the $Mg-H_2$ distance distribution for the ground state of $Mg(H_2)_{12}$, and Figure 10 gives the H_2-H_2 distance distribution for that system. (Ref. 30) Again, the results show

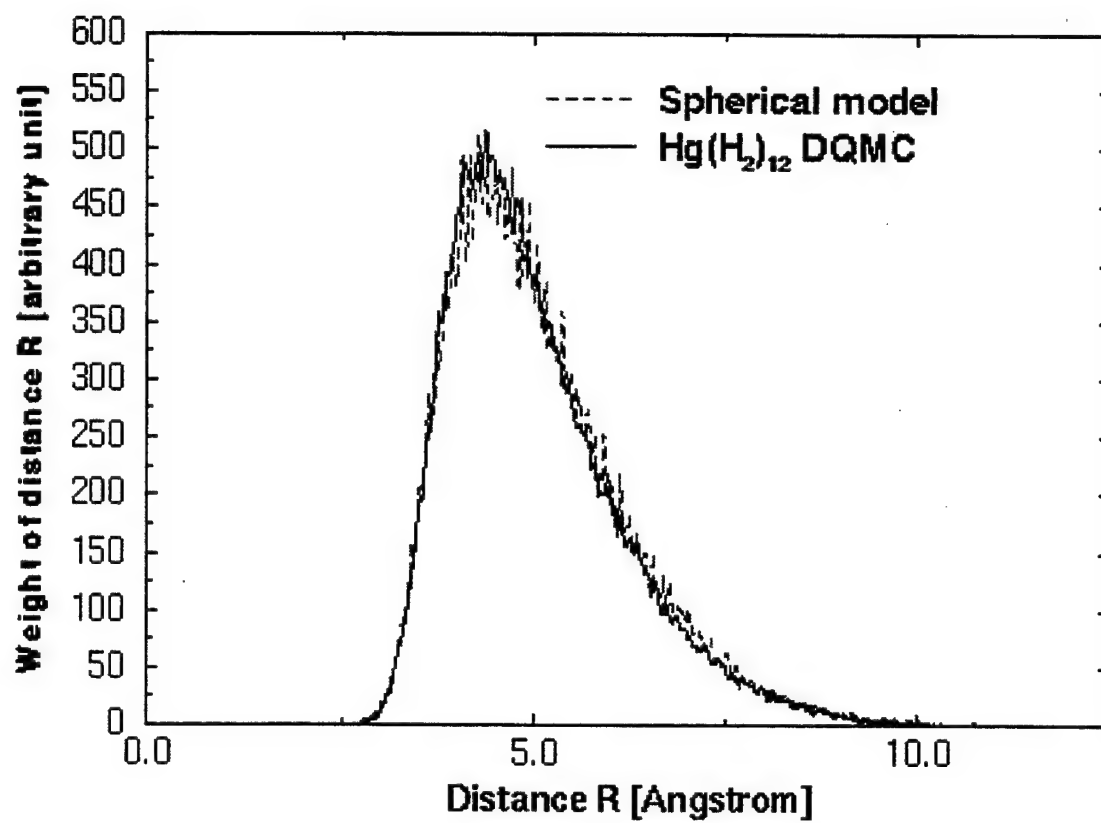


Figure 7
The H_2 -Hg Distance Distribution in the Ground State of $\text{Hg}(\text{H}_2)_{12}$

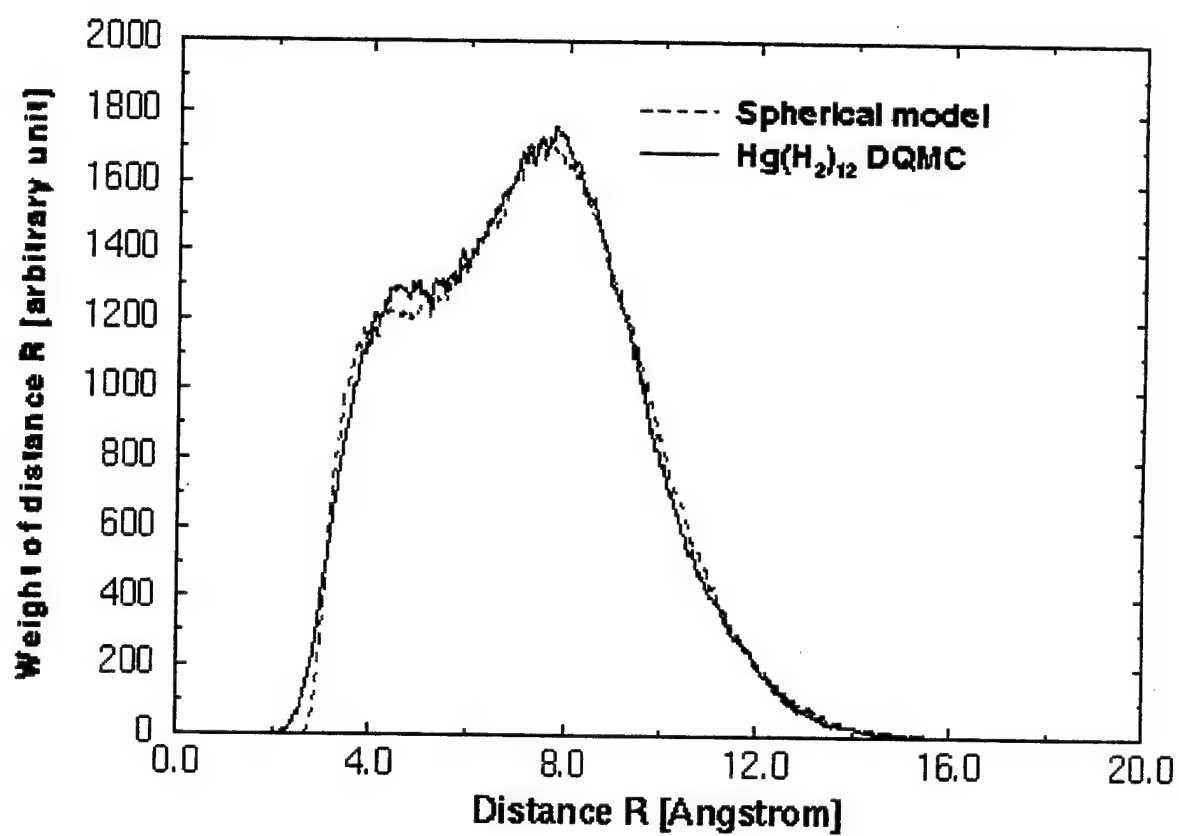


Figure 8
The H₂-H₂ Distance Distribution in the Ground State of Hg(H₂)₁₂

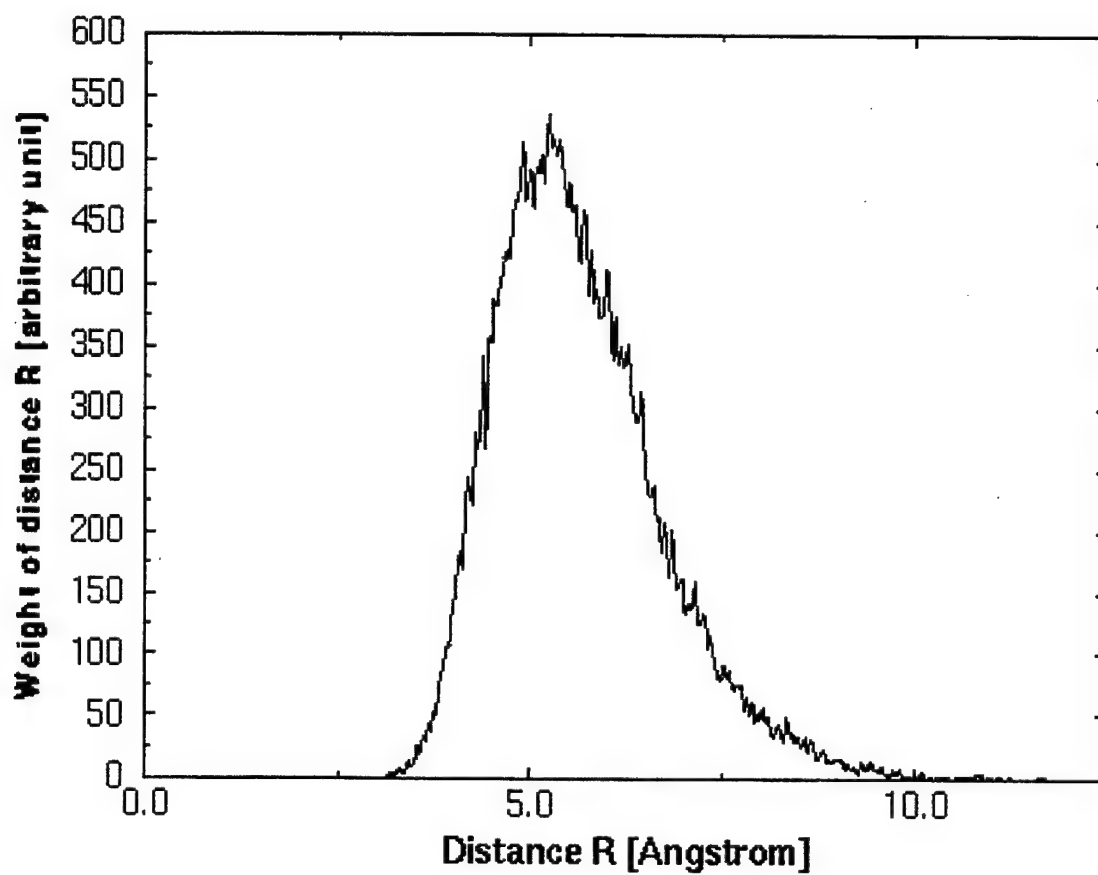


Figure 9
The H₂-Mg Distance Distribution in the Ground State of Mg(H₂)₁₂

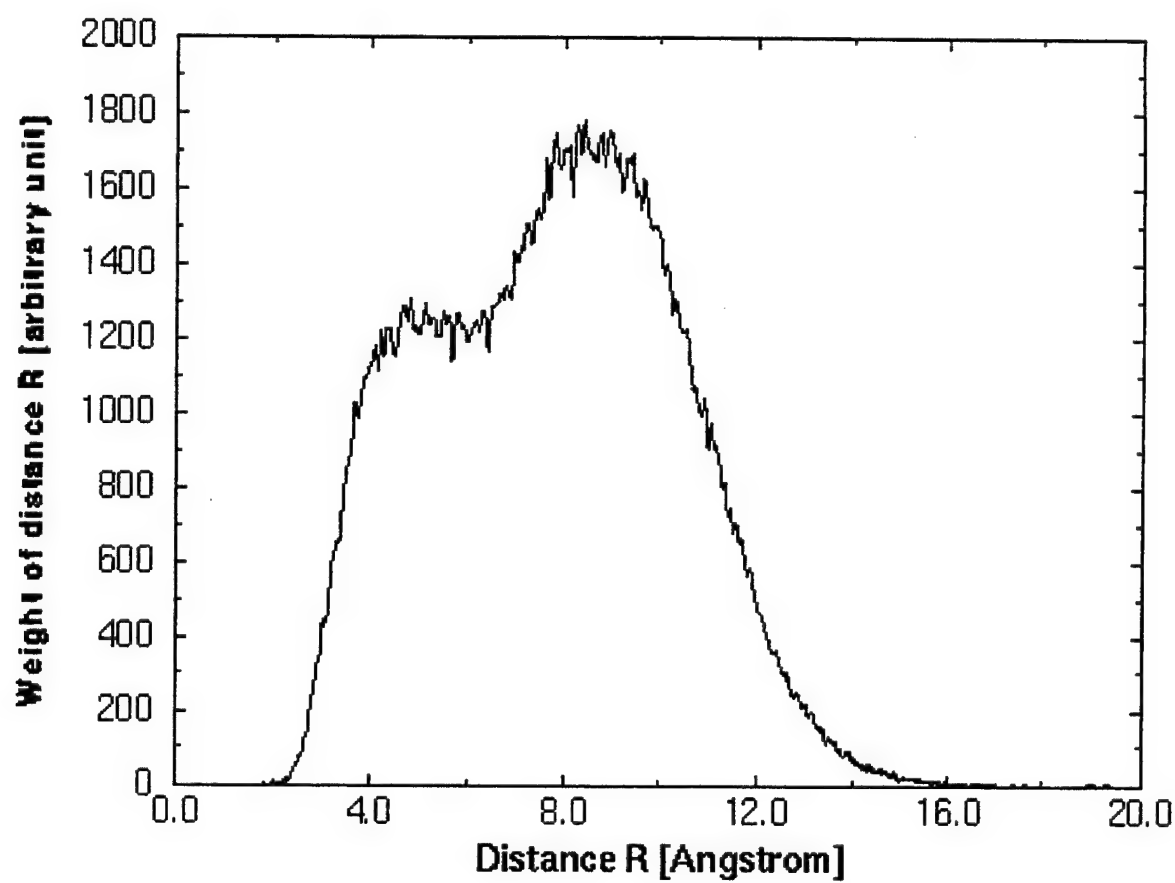


Figure 10
The H₂-H₂ Distance Distribution in the Ground State of Mg(H₂)₁₂ (From DQMC)

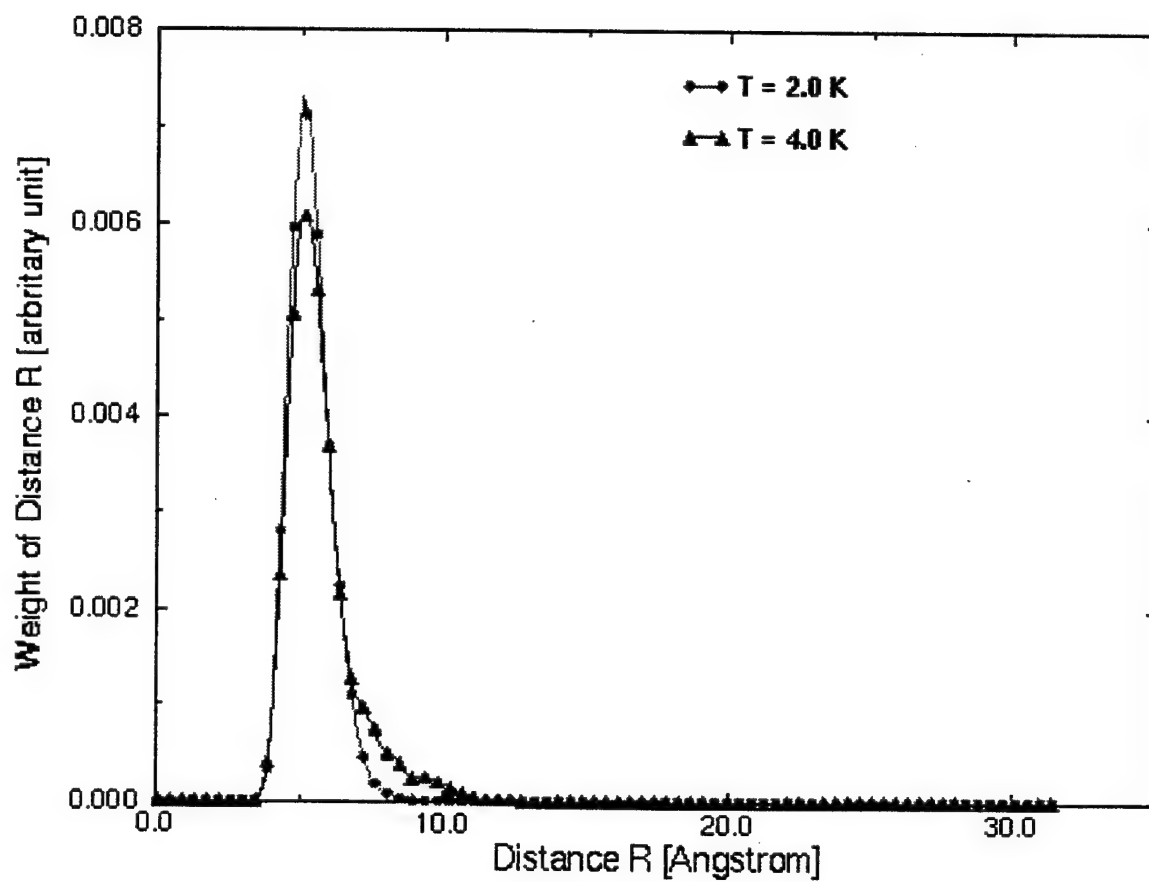


Figure 11
The Mg-H₂ Distance Distribution of the Mg(H₂)₁₂ at T=2K and at T=4K

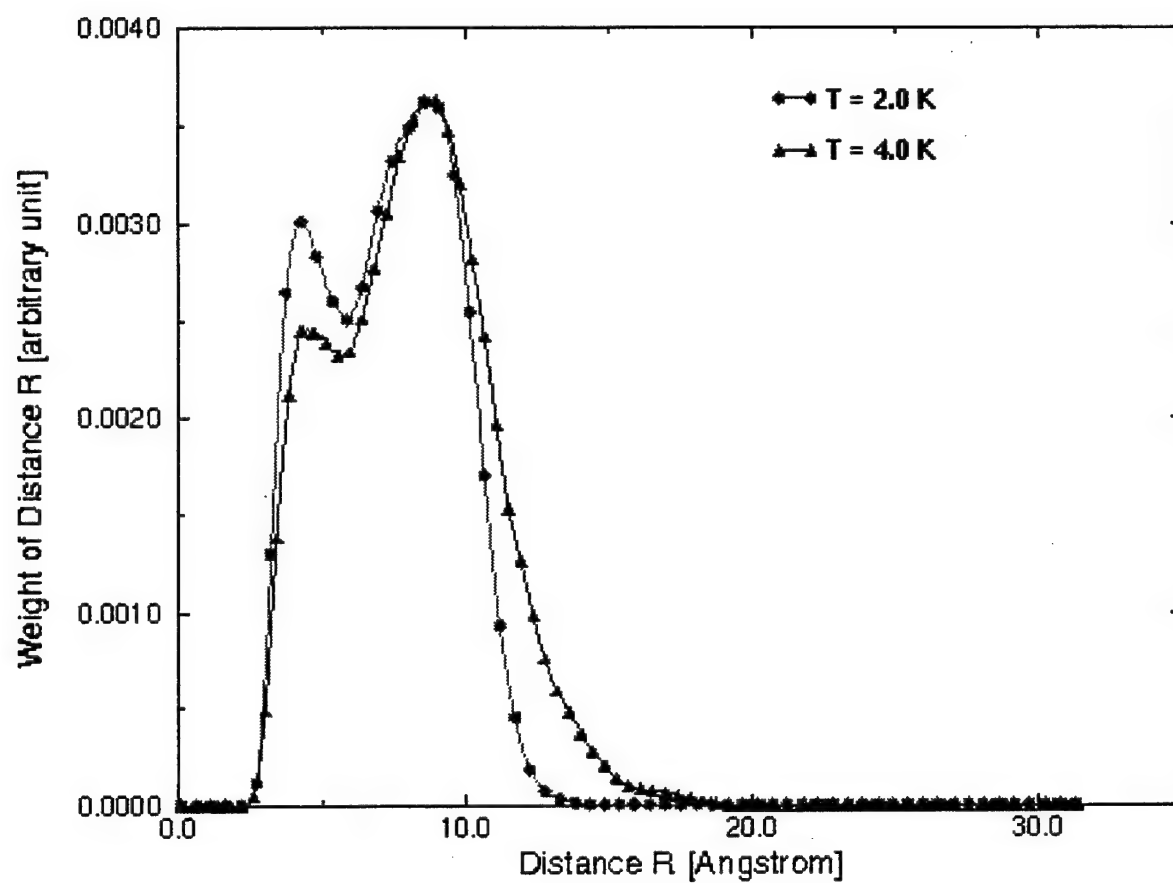


Figure 12
The H_2 - H_2 Distance Distribution for $\text{Mg}(\text{H}_2)_{12}$ at $T=2\text{K}$ and at $T=4\text{K}$

Scale of Figure: 23.8 Angstrom

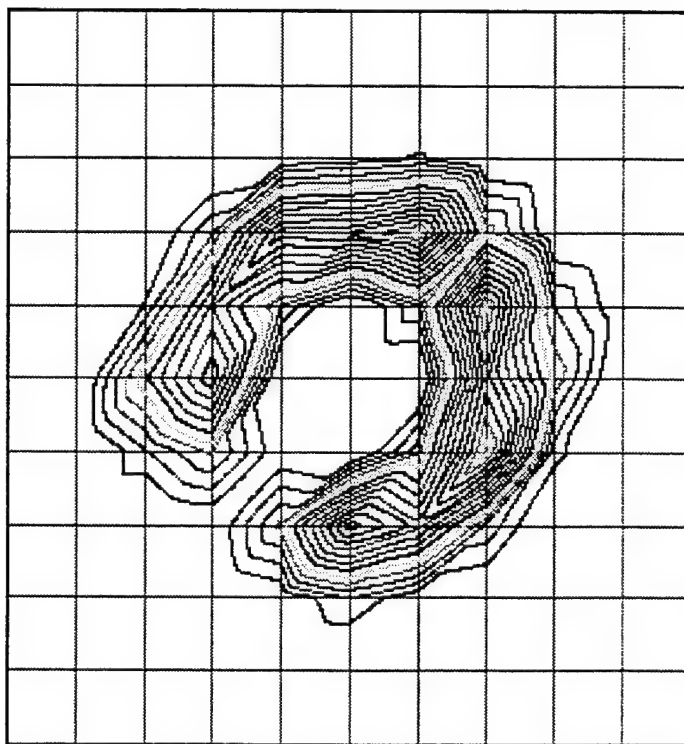


Figure 13
Density Contours for H₂ Molecules in a Plane Containing the Center of Mg, for the Cluster Mg(H₂)₁₂ at T=0K

the Mg atom to be "solvated" inside a "shell" of H₂ molecules. (Ref. 30) There is essentially zero probability to find the Mg at or outside the solvation shell, which therefore shields very well the Mg atom. This is already of importance in assessing the stability of Mg on solid hydrogen against recombination, etc.

(3) Temperature-dependence of the structure of Mg(H₂)_n: Figure 11 shows the Mg – H₂ distance distribution for Mg(H₂)₁₂ at $T=2\text{K}$ and $T=4\text{K}$. Figure 12 gives the H₂ – H₂ distance distribution in the same calculations. (Ref. 32) These results were obtained by using Feynman Path Integral Simulations. (Ref. 32) The results show that the structure of the cluster, while somewhat expanded in size, is as in the ground state: An Mg atom solvated inside a shell. The results show that this behavior is maintained until the evaporation temperature ($T=4.2\text{K}$) of this cluster is reached. These results suggest that in solid H₂, Mg should be "shielded" by the neighboring hydrogens, locked in its cage until $T=4\text{K}$ at least, and negligible diffusivity should be expected.

(4) Anisotropy of Mg(H₂)_n clusters: The structure of Hg(H₂)₁₂ is nearly isotropic. Figure 13 shows the density contour for H₂ molecules in a plane that contains the center of the Mg atom. The result is for $T=0\text{K}$. Clearly, the structure of Mg(H₂)₁₂ has an appreciable anisotropy, with a "hole" in the envelope of the H₂ molecules. This behavior of an anisotropic quantum cluster is maintained until the evaporation temperature of the cluster ($T=4.2\text{K}$), at least to a large extent. For Mg(H₂)₁₆, Mg(H₂)₁₇, Mg(H₂)₁₈, the first solvation shell around the Mg is complete, and the structure around the Mg is closer to isotropic, although not perfectly so.

(5) Vibrational wavefunction model, and vibrational properties of Hg(H₂)₁₂, Mg(H₂)₁₂: An analytical wavefunction model was fitted to the numerically calculated DQMC distribution. For the $n = 12$ clusters, the fitted wavefunction that worked well was:

$$\Psi(\mathbf{R}_1, \dots, \mathbf{R}_{12}, \mathbf{R}) = J(r_{i,j}; 1 \leq i \neq j \leq 12) \prod_{i=1}^{12} \chi(r_i) \quad (9)$$

where \mathbf{R}_i is the position vector of the i -th H₂ molecule, \mathbf{R} - the position vector of M, $r_{i,j} \equiv |\mathbf{R}_i - \mathbf{R}_j|$ is the distance between the i -th and j -th molecules, $r_i \equiv |\mathbf{R}_i - \mathbf{R}|$ is the distance between H₂(i) and M. For $\chi(r_i)$, the vibrational ground state of the M – H₂ dimer was used. J is a Jastrow factor (37) defined here by:

$$J(r_{i,j}; 1 \leq i \neq j \leq 12) = C \exp[-\sum_{i \neq j} \sum U_{rep}(r_{i,j})] \quad (10)$$

$$U_{rep}(r) = \left(\frac{\sigma}{r}\right)^{12} \quad (11)$$

C is determined by the normalization of the wavefunction and σ is the only free parameter used in fitting the wavefunction to the DQMC results. Trial wavefunctions of this type, and more elaborate ones, were employed in variational calculations of quantum clusters. (Ref. 25) Note that the procedure used here does not involve a variational approximation, but a fitting to DQMC results. The quality of the model, referred to in this report as "the spherical model" of M(H₂)₁₂ is shown in Figures 7 and 8 for M=Hg, is excellent. For M=Mg the fit is less desirable than for Hg, but also quite satisfactory. The wavefunction of Equations (10)-(12) offers a simple physical picture for the vibrational dynamics: Hg(H₂)₁₂ has two types of vibrations: "Radial" vibrations of H₂ versus Hg, and collective vibrations taking place on the sphere of the (H₂)₁₂ shell. This should be useful for the

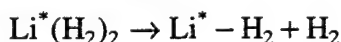
interpretation of future spectroscopy on such systems.

The results of this section suggest that Mg in solid H₂, because of the spontaneous solvation of Mg inside Mg(H₂)₁₂, is likely to prove a more advantageous material for HEDM than Li in hydrogen. It should be possible to prepare the material with higher concentrations of the dopant in the case of Mg, and the diffusivity of Mg should remain very low under 4K, preventing segregation. These results accomplished, together with those for B(H₂)_n, Tasks (1), (2) and (4) of the Program Plan.

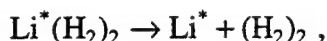
2.6 Photodynamics and Spectroscopy of Li(H₂)₂

The purpose of this part of the project was to calculate the dynamics in time following electronic excitation of a model of a doped hydrogen cluster, and to characterize its spectroscopic consequences. Electronic excitation of metal atoms in solid hydrogen and also in hydrogen clusters has emerged as an important experimental tool in the field, and calculations for a simple model system may help guide future experiments with regard to the main effects anticipated. The model chosen was the collinear cluster Li-H₂-H₂. The position of the Li in the end, corresponds to the fact that in real 3D Li(H₂)_n clusters, Li is outside the "droplet" of the H₂ molecules. The calculations were done by a time-dependent quantum wavepacket method. Since the system is a small one, a "conventional" grid method was used, rather than the novel CSP method, although later tests have shown that the CSP-based algorithm gives the same results. The system has Σ and Π-type excited states, and calculations for excitation into the Π state were carried out. Below is a summary of the results from Reference (40):

(1) There are two predissociation processes,



and



with the latter process having a much higher yield.

(2) A long predissociation time, of the order of $t \geq 10^4$ fs, was found for the excited cluster. Snapshots in time of the wavepacket calculated for the process are shown in Figure 14.

(3) The photoproduct Li* - H₂ is formed with highly excited final vibrational state distributions. The result is shown in Figure 15.

(4) A hybrid quantum-classical method was tested, in which the initial state is described quantum-mechanically, but the dissociation dynamics is treated classically. The conclusion was that for some properties (see Figure 15, for instance) this method does very well, but for the lifetimes and branching ratios it is severely in error, and quantum calculations must be used.

These results accomplish Task 6 of the Workplan.

2.7 Collision Dynamics and Dynamical Stability of Hydrogen Clusters

The survival probabilities of quantum clusters are data of importance for certain potential approaches that have been proposed for preparing HEDM propellants. To

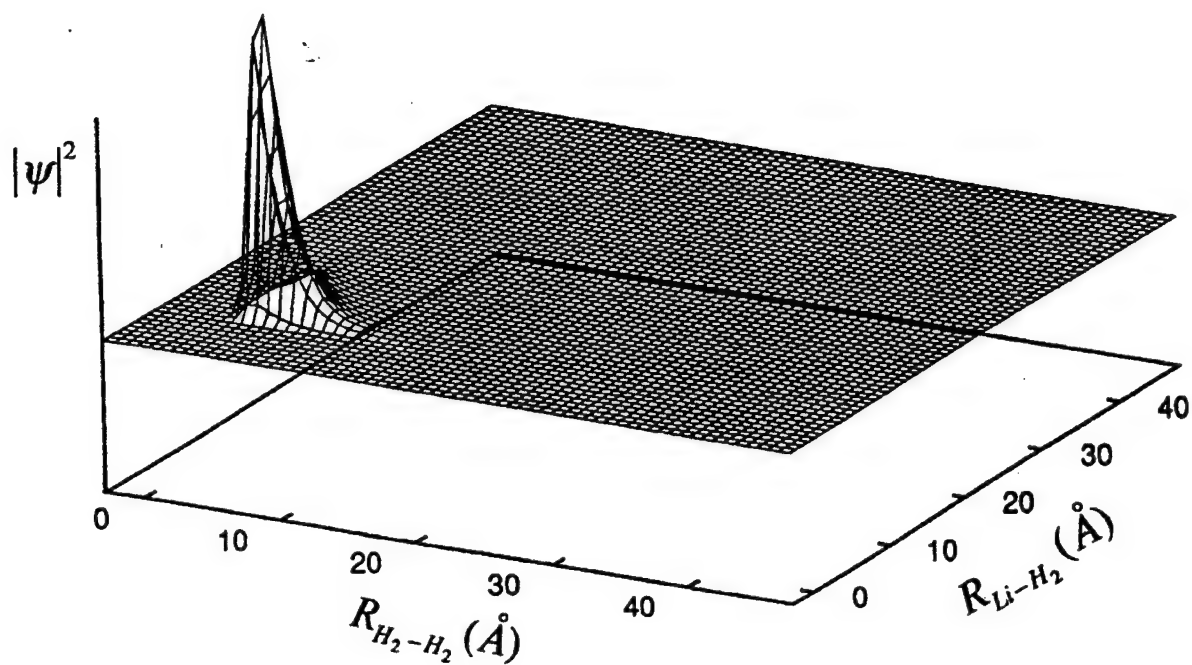


Figure 14a

Snapshot of the Time Evolution of the Wave Packet of $\text{Li}^*(\text{H}_2)_2$ After Photoexcitation. $t=0.0$ fs

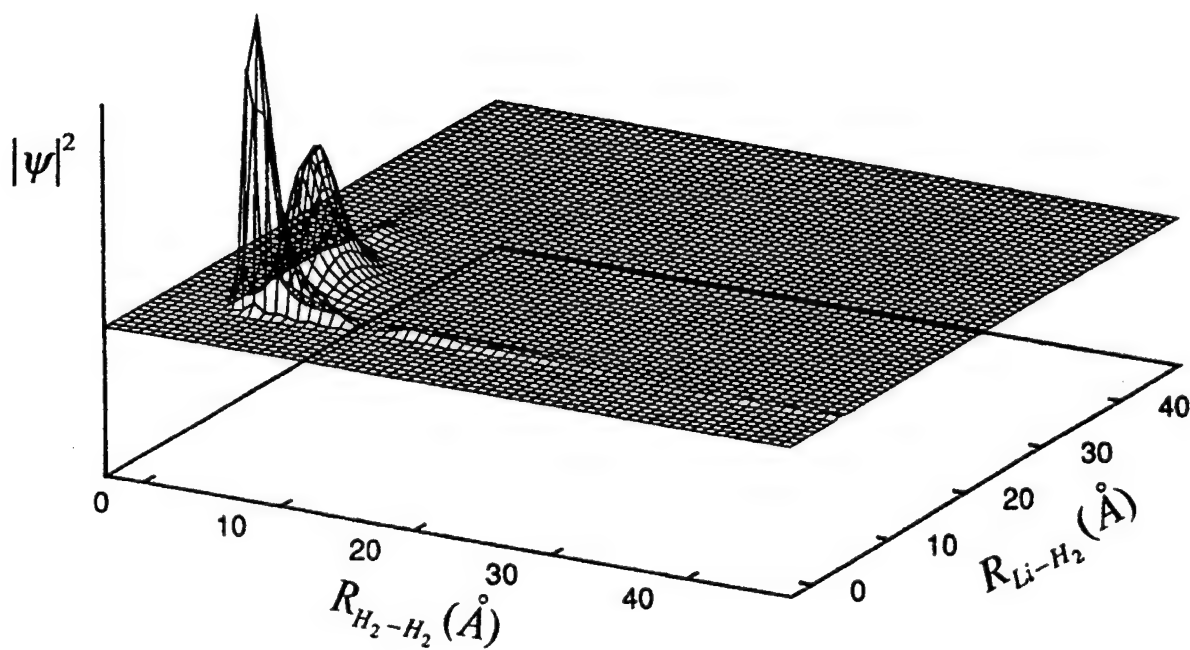


Figure 14b

Snapshot of the Time Evolution of the Wave Packet of $\text{Li}^*(\text{H}_2)_2$ After Photoexcitation
 $t=3600$ fs

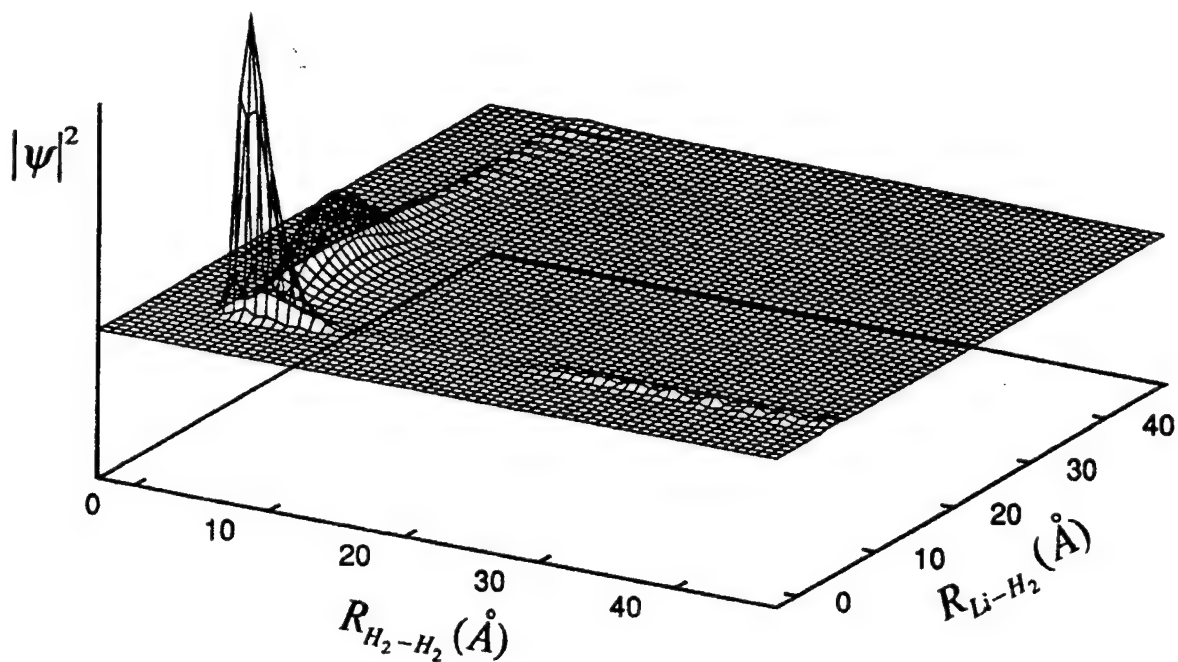


Figure 14c
Snapshot of the Time Evolution of the Wave Packet of $\text{Li}^*(\text{H}_2)_2$ After Photoexcitation
 $t=7200$ fs

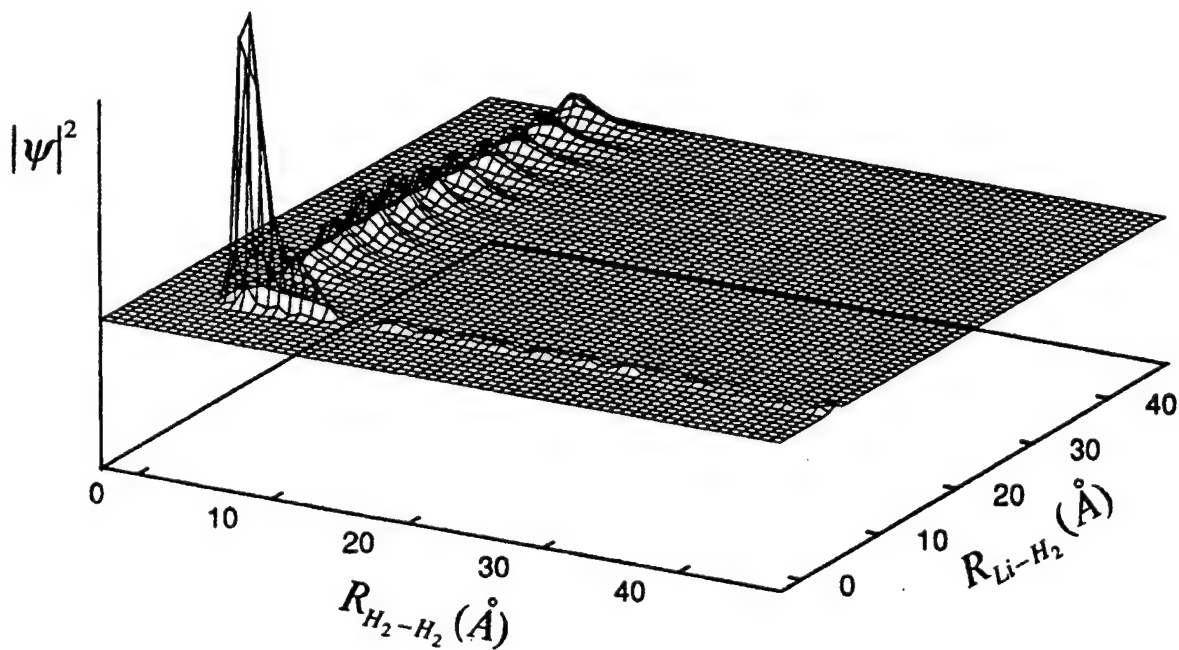


Figure 14d
Snapshot of the Time Evolution of the Wave Packet of $\text{Li}^*(\text{H}_2)_2$ After Photoexcitation
 $t=14400$ fs

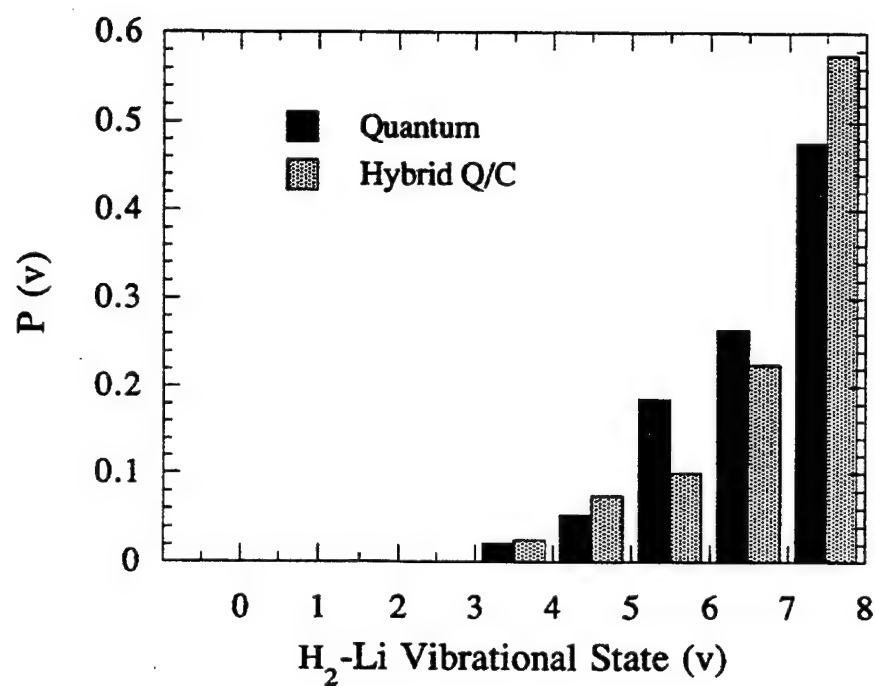


Figure 15
Final Vibrational State Distribution of the Dissociation Fragment $\text{Li}^* - \text{H}_2$ After the Photoexcitation

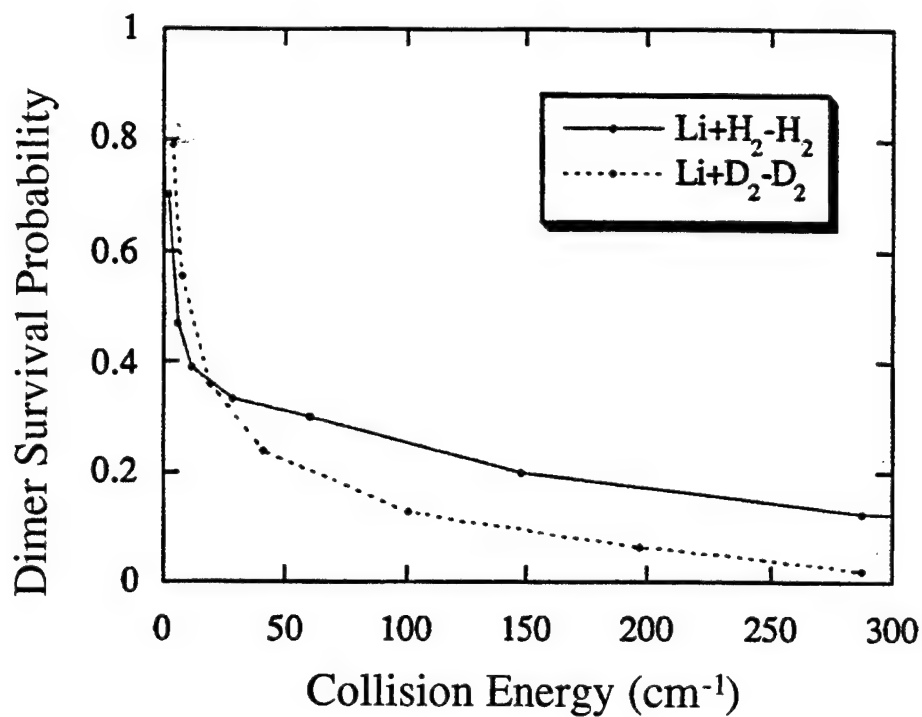


Figure 16
The Probability for Cluster Survival in Collinear Collisions of Li Atoms with (H₂)₂ and (D₂)₂

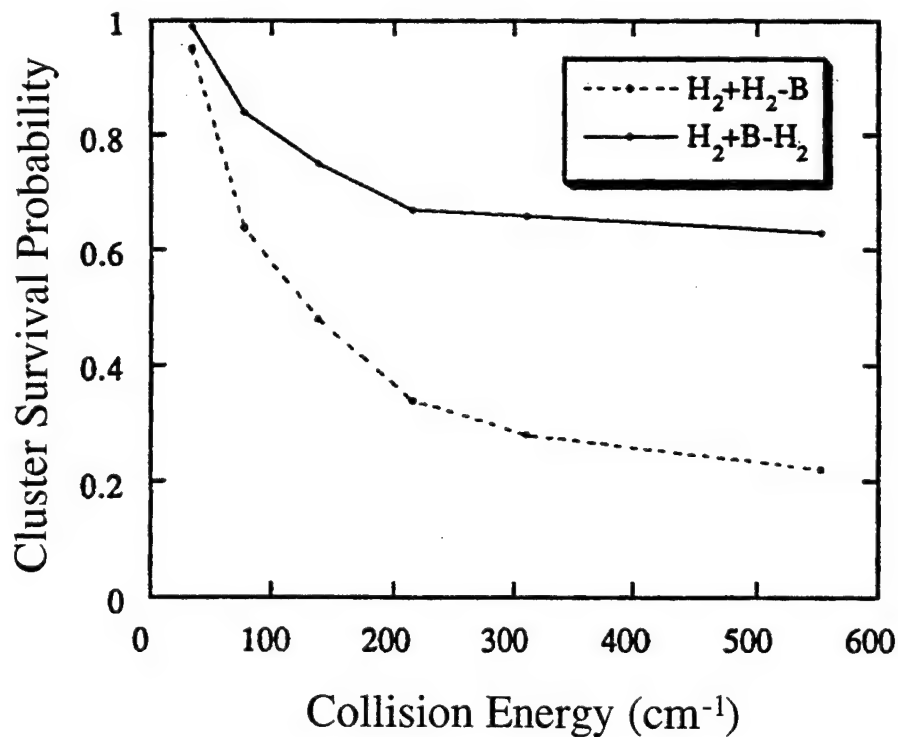


Figure 17
The Survival Probability of B-H₂ in Collinear Collisions with (H₂) Molecules

provide such data quantum calculations on the collision dynamics and survival probability in collisions for several clusters such as $(\text{H}_2)_2$, $\text{B} - \text{H}_2$, $(\text{H}_3)_2$, etc. were carried out, in collisions with H_2 molecules or with Li atoms. Figure 16 from Reference (15) gives the survival probabilities for $(\text{H}_2)_2$ and $(\text{D}_2)_2$ in collisions with Li atoms, as a function of collision energy. Surprisingly high survival probabilities are found, even for collision energies much greater than the (very weak) driving energy of the cluster. Figure 17 gives survival probabilities for $\text{H}_2\text{-B}$ in collisions with H_2 . We used a collinear model, and computed both the $\text{H}_2 + \text{H}_2 - \text{B}$ and the $\text{H}_2 + \text{B} - \text{H}_2$ types of impact. Again, very high survival probabilities are found. Analysis shows that the high probabilities are due to a quantum effect: Configurations in the collisions that are conducive to collision induced dissociation are classically quite likely, but have a much lower weight in quantum mechanics. Further analysis of the dynamics is given in Reference (15). The result shows an approach to making HEDM systems that depends on a high probability of survival (dynamical stability) of quantum clusters may be viable. This result accomplishes Task 5 of the (revised) Program Plan.

2.8 Photodynamics of Mg Atoms in Solid Hydrogen

Although this part of the work is not completed yet, the results already obtained on this topic are important, and contribute to the success of the project. Preliminary calculations on the $S \rightarrow P$ excitation of magnesium atoms in solid hydrogen were performed. The calculations were carried out by using the time-dependent quantum-mechanical method, based on the CSP approximation, that was developed in the present project. A simulation box that included 54 hydrogen molecules with periodic boundary conditions, at the density of hydrogen at normal pressure for $T \rightarrow 0\text{K}$ was used. The system was "doped" with Mg atoms by removing 4 hydrogen molecules from the center of the box, and inserting an Mg atom instead. Estimates indicate that the replacement of 4 hydrogen molecules by an Mg atom is energetically the most favorable. Diffusion Quantum Monte Carlo (DQMC) on this system of one Mg surrounded by 50 hydrogens, and with periodic boundary conditions were then carried out. A model wavefunction was then fitted to the DQMC results, along the lines of the model wavefunction fitting for $\text{Mg}(\text{H}_2)_{12}$, described in section 5. To model the $S \rightarrow P$ excitation, the above ground state wavefunctions were used as the initial state, and began to propagate it on the excited potential surface. Excitation into the singlet state was considered. Tests have shown that the simulation box with 50 hydrogen molecules is too small, and the results can therefore not be trusted, at least quantitatively. There are indications that for a simulation box with 100 hydrogen molecules the size of the box will be sufficient for physically realistic results, at least for short times. The qualitative, or semiquantitative, results that nevertheless merit attention and may remain valid for the larger simulation box are:

- (1) Following excitation, photoinduced mobility of the Mg is found with high yield: Nearly 35% of the Mg^* atoms migrate from the original cage to a neighboring cage.
- (2) For the Mg^* atoms that have not migrated, highly excited cage vibrations take place. These vibrations are mostly "radial" with the H_2 molecules oscillating against the Mg. The vibrations are coherent for $t \sim 400$ fs at least, and decay slowly due to coupling with other H_2 molecules.
- (3) Appreciable non-adiabatic transitions are seen already for $t \geq 600$ fs. In these events, the electronic population, initially in the highest P -state, relaxes in part to the

intermediate electronic state. There is no significant electronic population in the lowest electronic state, at least for $t \leq 800$ fs.

It should be extremely useful to study the system of Mg in solid hydrogen by ultra-fast time-resolved spectroscopy, to observe both the photo-diffusion and the nonadiabatic transitions. Data on electronic spectroscopy of Mg in solid H_2 was reported by Presser. (Ref. 41)

These results contribute to achieving Task 2 of the Program Plan of our research, and with them also Task 8 is, in part, accomplished.

2.9 Structural and Thermodynamic Properties of Hydrogen/Rare Gas Mixtures on Surfaces

This result touches only in a marginal way on our project and also there is only a very preliminary result. Nevertheless, because of the scientific interest, it is mentioned here. It was suggested almost three years ago that monolayers which are mixtures of H_2 with Rg, should have disordered structures that are very different from corresponding rare gas mixtures. For instance, mixtures of Xe+Kr on Pt are substitutionally disordered, but crystalline - periodic over a wide range of T . For H_2 /Ar mixtures on a flat surface we expected other types of disorder, and a strong effect of T on the disordered type. This was due to the fact that for Rg, the van der Waals radii play the critical role and determine the disordered type, while for H_2 , the de Broglie wavelength is the key parameter.

A cooperation was established with P. Zeppenfeld (Jülich) and M. Bienfait (Marseille) which carried out neutron diffraction experiments on H_2 +Ar on graphite, in Grenoble, France. Early results suggest indeed a possibility of a novel type disorder behavior.

The results may be useful in understanding the structures and thermodynamic stability of H_2 +M mixtures (M-doping material) and high mixing ratios.

3. WORK IN PROGRESS

Calculations are in progress on the dynamics following electronic excitation of Mg atoms in solid hydrogen. Results were reported in Section (2.8), but the number of H_2 molecules used in the simulations was, by the current evidence, too small. Simulations of Mg in a sample of over 108 hydrogen molecules (with periodic boundary conditions) should be necessary for realistic physical results. The calculations carried out now are time-dependent quantum mechanical simulations, by the method developed in this project. Properties such as photoinduced mobility, electronic energy, vibrational relaxation (of the excited "spot" consisting of the Mg atom and the surrounding cage), and electronic adsorption spectroscopy are being computed.

Another calculation still in progress is the continuation of the calculations for $B(H_2)_n$ clusters, with $n = 1, \dots, 8$. Currently, DQMC calculations of $B(H_2)_n$ with $n \approx 100$ are being performed along with calculations for B in solid H_2 , with periodic boundary conditions. The aims of the calculations are structural properties, energetic stability, and consequences for diffusion. Calculations of electronic spectra are also being contemplated.

4. RECOMMENDATIONS AND CONCLUSIONS FOR THE HEDM PROJECT

Included here are only a few main recommendations. More detailed, technical conclusions and recommendations are mentioned in the Summary and in the Results Sections.

- (1) Focussing with high priority on developing boron in solid hydrogen as a HEDM propellant. By the aspects studied, this is by far the most promising HEDM candidate.
- (2) Mg in hydrogen seems, by the results of this research, to have important advantages over Li in hydrogen as a potential HEDM propellant. It appears that now Li in H₂ is getting more attention. By the reported results, Mg in H₂ has better stability and can be built up to higher doping concentrations. This suggests a change in priority. Boron in hydrogen seems, nevertheless, much more promising than either of these.
- (3) The Phillips Laboratory should consider time-resolved spectroscopy as a new, additional tool for in-house experiments to characterize HEDM systems, especially as to dynamical properties, and
- (4) The Phillips Laboratory should consider adopting time-dependent quantum simulations as a tool for supporting some of the experiments.

5. REFERENCES

- (1) P. Carrick, "Theoretical Performance of Atomic and Molecular Additives to Solid Hydrogen," Proceedings of the HEDM Contractors Conference, Jun 1993. Edited by T.L. Thompson, Phillips Laboratory, Air Force Materiel Command, Nov 1993, pp. 412-418.
- (2) P. Jungwirth and R.B. Gerber, "Quantum Dynamics of Large Polyatomic Systems Using a Classically Based Separable Potential Method," *J. Chem. Phys.*, **102**, 1995, pp. 6046.
- (3) P. Jungwirth and R.B. Gerber, "Quantum Dynamics of Many-Atom Systems by the Classically Based Separable Potential (CSP) Method: Calculations for I(Ar)₁₂ in Full Dimensionality," *J. Chem. Phys.*, **102**, 1995, pp. 8855.
- (4) P. Jungwirth and R.B. Gerber, "Quantum Dynamics Simulations of Nonadiabatic Processes in Many-Atom Systems: Photoexcited Ba(Ar)₁₀ and Ba(Ar)₂₀ Clusters," *J. Chem. Phys.*, **104**, 1996, pp. 5803.
- (5) P. Zeppenfeld, O. Wilkes, M. Bienfait and R.B. Gerber (to be published, for address to obtain, see Ref. 30.)
- (6) M.P. Allen and D.J. Tildesley, "Computer Simulations of Liquids," (1987, Clarendon, Oxford.)
- (7) R. Kosloff, "Time-Dependent Quantum-Mechanical Methods for Molecular Dynamics," *J. Phys. Chem.*, **92**, 1988, pp. 2087.
- (8) R.B. Gerber and M.A. Ratner, "Self-Consistent Field Methods for Vibrational Excitation in Polyatomic Systems," *Adv. Chem. Phys.*, **70**, 1988, pp. 97.
- (9) J.C. Tully, "Molecular Dynamics with Electronics Transitions," *J. Chem. Phys.*, **93**, 1990, pp. 1061.
- (10) J.P. Visticot, P. de Pujo, J.M. Mestdagh, A. Lallermont, J. Berlande, O. Sublemontier, P. Menadier and J. Cuvellier, "Experiment vs. Molecular Dynamics

- Simulation: Spectroscopy of $\text{Ba}(\text{Ar})_n$ Clusters," *J. Chem. Phys.*, **100**, 1994, pp. 158.
- (11) B. Schilling, M.-A. Gaveau, O. Sublemontier, J.M. Mestdagh, J.P. Visticot, X. Biquar and J. Berlande, "Photodesorption Dynamics of Ba Atoms from Large Ar Clusters," *J. Chem. Phys.*, **101**, 1994, pp. 5722.
 - (12) A.I.Krylov, R.B. Gerber, M.A. Gaveau, J.M. Mestdagh, B. Schilling and J.P. Visticot, "Spectroscopy, Polarization and Non-Adiabatic Dynamics of Electronically Excited $\text{Ba}(\text{Ar})_n$ Clusters: Theory and Experiment," *J. Chem. Phys.*, **104**, 1996, pp. 3651.
 - (13) M.E. Fajardo, "Matrix Isolation Spectroscopy of Metal Atoms Generated by Laser Ablation. II. The Li/Ne, Li/D₂ and Li/D₂ Systems," *J. Chem. Phys.*, **98**, 1993, pp. 110.
 - (14) M.E. Fajardo, S. Tam, T.L. Thompson and M.E. Cordonnier, "Spectroscopy and Reactive Dynamics of Atoms Trapped in Molecular Hydrogen Matrices," *Chem. Phys.*, **189**, 1994, pp. 351.
 - (15) Z. Li and R.B. Gerber, "Validity of the Time-Dependent Self-Consistent Field (TDSCF) Approximation for Non-Stationary Vibrational State of Quantum Clusters," *Chem. Phys. Lett.* (in press.)
 - (16) N. Makri and W.H. Miller, "Time-Dependent Self-Consistent Field (TDSCF) Approximation for a Reaction Coordinate Coupled to a Harmonic Bath: Single and Multiple Configuration Treatments," *J. Chem. Phys.*, **87**, 1987, pp. 5781.
 - (17) J. Compos-Martinez and R.D. Coalson, "Adding Configuration Interaction to the Time-Dependent Hartree Grid Approximation," *J. Chem. Phys.*, **93**, 1990, pp. 4740.
 - (18) H.-D. Meyer, U. Manthe and L.S. Cederbaum, "The Multi-Configurational Time-Dependent Hartree Approach," *Chem. Phys. Lett.*, **165**, 1990, pp. 73.
 - (19) J.-Y. Fang and H. Guo, "Multiconfiguration Time-Dependent Hartree Studies of the Cl_2Ne Vibrational Predissociation Dynamics," *J. Chem. Phys.*, **102**, 1995, pp. 1944.
 - (20) L. Liu, J.-Y. Fang and H. Guo, "How Many Configurations are Needed in a Time-Dependent Hartree Treatment of the Photodissociation of $\text{ICN}^?$," *J. Chem. Phys.*, **102**, 1995, pp. 2404.
 - (21) Z. Li and R.B. Gerber, "Treatment of Zero-Point Motions in Cluster Dynamics: Semiclassical Time-Dependent Self-Consistent-Field Simulation of $(\text{Ne})_N$," *J. Chem. Phys.*, **99**, 1993, pp. 8637.
 - (22) E. Fredj, R.B. Gerber and M.A. Ratner, "Semiclassical Molecular Dynamics Simulations of Low-Temperature Clusters: Applications to $(\text{Ar})_{13}$; $(\text{Ne})_{13}$; $(\text{H}_2\text{O})_n$, $n=2,3,5$," *J. Chem. Phys.* (in press.)
 - (23) J.B. Anderson, "A Random-Walk Simulation of the Schrödinger Equation: H_3^+ ," *J. Chem. Phys.*, **63**, 1975, pp. 1499.
 - (24) M.A. Suhm and R.O. Watts, "Quantum Monte Carlo Studies of Vibrational States in Molecules and Clusters," *Phys. Rep.*, **204**, 1991, pp. 293.
 - (25) R.N. Barnett and K.B. Whaley, "Molecules in Helium Clusters: $\text{SF}(\text{He})_N$," *J. Chem. Phys.*, **99**, 1993, pp. 9730.
 - (26) M.A. McMahon, R.N. Barnett and K.B. Whaley, "Rotational Excitations of Quantum Liquid Clusters: $(\text{He})_n(\text{H}_2)_n$," *J. Chem. Phys.*, **99**, 1993, pp. 8816.

- (27) V. Buch, "Treatment of rigid Bodies by Diffusion Monte Carlo: Application to the para - $\text{H}_2 \cdots (\text{H}_2\text{O})$ and Ortho - $\text{H}_2 \cdots (\text{H}_2\text{O})$ Clusters," *J. Chem. Phys.*, **97**, 1992, pp. 726.
- (28) Z. Bacic, M. Kennedy-Manduziuk, J.W. Moskowitz and K.E. Schmidt, " He_2Cl_2 and $(\text{He})_3\text{Cl}_2$ van der Waals Clusters: A Quantum Monte Carlo Study," *J. Chem. Phys.*, **97**, 1992, pp. 64722.
- (29) A. Vegiri, M.H. Alexander, S. Gregurick, A.B. McCoy and R.B. Gerber, "Quantum Monte Carlo Studies of Small $\text{B}(\text{H}_2)_n$ Clusters," *J. Chem. Phys.*, **101**, 1994, pp. 2577.
- (30) S. Broude and R.B. Gerber, "Solvation of Metal Atoms in Quantum Clusters: Structural and Vibrational Properties of $\text{Mg}(\text{H}_2)_{12}$, $\text{Mg}(\text{H}_2)_{12}$," *Chem. Phys. Lett.* (Submitted. To obtain, contact R.B. Gerber, 516 Physical Sciences 1, University of California, Irvine, Irvine, California 92697-2025.)
- (31) D. Scharf, G.J. Martyna and M.L. Klein, "Path-Integral Monte Carlo Study of a Lithium Impurity in Para-Hydrogen: Clusters and the Bulk Liquid," *J. Chem. Phys.*, **99**, 1993, pp. 8997.
- (32) E. Fredj, S. Broude, J.O. Jung and R.B. Gerber (To be published. For more information contact R.B. Gerber at the address in Ref. 30.)
- (33) D. Chandler and P. Wolynes, "Exploiting the Isomorphism Between Quantum Theory and Classical Statistical Mechanics of Polyatomic Fluids," *J. Chem. Phys.*, **74**, 1981, pp. 4078.
- (34) B. De Raedt, M. Sprik and M.C. Klein, "Computer Simulation of Muonium in Water," *J. Chem. Phys.*, **80**, 1984, pp. 5719.
- (35) M.H. Alexander, "Adiabatic and Approximate Diabatic Potential Energy Surfaces for the $\text{B}(\text{H}_2)$ van der Waals Molecule," *J. Chem. Phys.*, **99**, 1993, pp. 6014.
- (36) D. Scharf, G.J. Martyna, D. Li, G.A. Voth and M.L. Klein, "Nature of Lithium Trapping Sites in the Quantum Solids Para-Hydrogen and Ortho-Deuterium," *J. Chem. Phys.*, **99**, 1993, pp. 9013.
- (37) J.O. Jung and R.B. Gerber (Unpublished report. For more information contact R.B. Gerber at the address in Ref. 30.)
- (38) G. Chaban and M.D. Gordon, *J. Chem. Phys.* (in press.)
- (39) T.R. Koehler, "Dynamical Properties of Solids," edited by G.K. Merton and A.A. Maradudin, Vol. 2, pp. 1 (1975, North Holland, Amsterdam.)
- (40) Z. Li and R.B. Gerber, "Electronic Excitation Dynamics of $\text{Li}(\text{H}_2)_2$: Dissociation Mechanisms, Lifetimes, and the Validity of a Hybrid Quantum/Classical Approach," *J. Chem. Phys.*, **102**, 1995, pp. 4056.
- (41) N. Presser, "Spectroscopy of Mg in Hydrogenic Matrices," *Chem. Phys. Lett.*, **199**, 1992, pp. 10.

6. LIST OF PUBLISHED ARTICLES FROM THE RESEARCH PROJECT

1. Z. Li and R.B. Gerber
"Treatment of Zero-Point Motions in Cluster Dynamics: Semiclassical Time-Depended Self-Consistent Field Simulations of $(\text{Ne})_N$ "
J. Chem. Phys., **99**, 1993, pp. 8637-8643.
2. A. Vegiri, M.H. Alexander, S. Gregurick, A.B. McCoy and R.B. Gerber
"Quantum Monte Carlo Studies of Small $\text{B}(\text{H}_2)_n$ Clusters"
J. Chem. Phys., **101**, 1994, pp. 2577-2591.
3. Z. Li and R.B. Gerber
"Survival of Weakly-Bound Quantum Clusters in Collisions with Atoms"
Chem. Phys. Lett., **229**, 1994, pp. 650-656.
4. A.I. Krylov, R.B. Gerber and V.A. Apkarian
"Adiabatic Approximation and Non-Adiabatic Effects for Open-Shell Atoms in an Inert Solvent: F Atoms in Solid Kr"
Chem. Phys. Lett., **189**, 1994, pp. 261-272.
5. A.I. Krylov and R.B. Gerber
"Reorientation Dynamics of Electronic Orbitals in Condensed Phases"
Chem. Phys. Lett., **231**, 1994, pp. 395-400.
6. Z. Li and R.B. Gerber
"Electronic Excitation Dynamics of $\text{Li}(\text{H}_2)_2$: Dissociation Mechanisms, Lifetimes and the Validity of a Hybrid Quantum/Classical Approach"
J. Chem. Phys., **102**, 1995, pp. 4056-4062.
7. P. Jungwirth and R.B. Gerber
"Quantum Dynamics of Large Polyatomic Systems Using a Classically-Based Separable Potential Method"
J. Chem. Phys., **102**, 1995, pp. 6046-6056.
8. P. Jungwirth and R.B. Gerber
Quantum Dynamics of Many-Atom Systems by the Classically-Based Separable Potential (CSP) Method: Calculations for $\text{I}(\text{Ar})_{12}$ in Full Dimensionality"
J. Chem. Phys., **102**, 1995, pp. 8855-9964.
9. Z. Li and R.B. Gerber
"The Validity of the Time-Dependent Self-Consistent Field (TDSCF) Approximation for Non-Stationary Vibrational Bound States of Quantum Clusters"
Chem. Phys. Lett., **243**, 1995, pp. 257-263.
10. P. Jungwirth and R.B. Gerber
"Quantum Dynamics Simulations of Non-Adiabatic Processes in Many-Atom Systems: Photoexcited $\text{Ba}(\text{Ar})_{10}$ and $\text{Ba}(\text{Ar})_{20}$ Clusters"
J. Chem. Phys., **104**, 1996, pp. 5803-5814.
11. S. Broude and R.B. Gerber
"Solvation of Metal Atoms in Quantum Clusters: Structural and Vibrational Properties of $\text{Mg}(\text{H}_2)_{12}$, $\text{Mg}(\text{H}_2)_{12}^+$ "
Chem. Phys. Lett. (submitted.)

7. INVITED LECTURES AT INTERNATIONAL CONFERENCES ON RESULTS FROM THE PROJECT

- (1) At: Gordon Conference on Vibrational Spectroscopy, Wolfeboro, NH, August 1994.
- (2) At: ACS Symposium on Dynamics in Condensed Phases, Washington, DC, August 1994.
- (3) At: MOLEC X Conference, Salamanca, Spain, September 1994.
- (4) At: SPIE Conference, San Diego, July 1995.
- (5) At: Femtosecond Chemistry, Lausanne, Switzerland, September 1995.
- (6) At: 10th SAP Conference, in Engelberg, Switzerland, January 1996.
- (7) To be given at: Conference on Molecular Reaction Dynamics in Condensed Phases, Newport Beach, February 1996.
- (8) To be given at: Symposium on Quantum Dynamics of Molecular Processes, Freiburg, Germany, February 1996.
- (9) To be given at: Israel-Czech Republic Binational Symposium on Chemical Dynamics, April 1996.
- (10) To be given at: Gordon Conference on Clusters, Braga, Italy, May 1996.
- (11) To be given at: International Conference on the Theory of Clusters, Wisconsin, September 1996.

In addition, I gave oral presentations at the following HEDM meetings:

HEDM Conference at Woods Hole, June 1993;

HEDM Conference at CalNeva, June 1994;

HEDM Conference at Woods Hole, June 1995.

Further, I gave lectures based on results from this project at the following universities:

Tel-Aviv University (1994); The Technion - Israel Institute of Technology (1994); Universite de Lausanne (1995); Freie Universität, Berlin (1995); University of Bordeaux, France (1994); Max-Planck-Institut, Göttingen (1995); University of Southern California (1995); University of Illinois, Urbana (Beckmann Institute) (1995).

8. CONTRIBUTION OF THE PROJECT TO THE TRAINING OF MAN-POWER IN THE HEDM FIELD

The following research students and postdoctoral fellows took part in this research, and got training in HEDM topics:

- (1) Dr. Zhiming Li (Nationality: PRC, permanent resident of the USA): Did postdoctoral research at UC Irvine on this project. Is currently doing postdoctoral research with Prof. Apkarian at UCI, also on HEDM topics.
- (2) Dr. Anne B. McCoy (US Nationality): Did postdoctoral research at UCI on the HEDM project. Dr. McCoy is currently Assistant Professor of Chemistry at Ohio State University.
- (3) Dr. Pavel Jungwirth (Czech Nationality): Did postdoctoral research at UCI on topics of the project. He currently holds a faculty position at the Heyrovsky Institute of the Czech Academy of Sciences.
- (4) Dr. Burkhard Schmidt (German Nationality): Did postdoctoral research on topics of the project. Currently he holds a junior faculty position at the Freie Universität, Berlin.
- (5) Joon O. Jung (US Nationality): Has done part of his graduate research on HEDM topics. Jung is currently a Ph.D. student with the PI (RBG) at UC, Irvine.
- (6) Sharon Broude (Israeli Nationality): Has done part of her graduate research on HEDM topics. Broude is a Ph.D. student with the PI (RBG) at The Hebrew University of Jerusalem.